NAVAL SHIP RESEARCH AND DEVELOPMENT CENTER
Washington, D.C. 20034

THEORETICAL PERFORMANCE OF A PURE JET FLAP ROTOR AT HIGH ADVANCE RATIOS

by

Robert M. Williams and Charles L. Bernitt

Approved for public release;
distribution unlimited.

AVIATION AND SURFACE EFFECTS DEPARTMENT

December 1970 Technical Note AL-189

Technical Note AL-189

THEORETICAL PERFORMANCE OF A PURE JET FLAP ROTOR
AT HIGH ADVANCE RATIOS

UNCLASSIFIED

Security Classification

DOCUMENT CONTROL DATA - R & D

(Security classification of title, body of abstract and indexing annotation must be entered when the overall report is classified)

1. ORIGINATING ACTIVITY (Corporate author)
Aviation and Surface Effects Department
Naval Ship Research and Development Center
Washington, D. C. 20034

2a. REPORT SECURITY CLASSIFICATION
UNCLASSIFIED

2b. GROUP

3. REPORT TITLE
THEORETICAL PERFORMANCE OF A PURE JET FLAP ROTOR AT HIGH ADVANCE RATIOS

4. DESCRIPTIVE NOTES (Type of report and inclusive dates)
Technical Note

5. AUTHOR(S) (First name, middle initial, last name)
Robert M. Williams and Charles L. Bernitt

6. REPORT DATE	7a. TOTAL NO. OF PAGES	7b. NO. OF REFS
December 1970	50	4

8a. CONTRACT OR GRANT NO.	9a. ORIGINATOR'S REPORT NUMBER(S)
b. PROJECT NO. WF 32.421.202	Technical Note AL-189
c.	9b. OTHER REPORT NO(S) (Any other numbers that may be assigned this report)
d. 63Y-700	

10. DISTRIBUTION STATEMENT
Approved for public release; distribution unlimited.

11. SUPPLEMENTARY NOTES	12. SPONSORING MILITARY ACTIVITY
	Commander Naval Air Systems Command (320) Department of the Navy Washington, D. C. 20360

13. ABSTRACT

The theoretical performance of a jet flap rotor at advance ratios greater than 1.0 is examined. The rotor is four bladed with purely elliptical airfoils of fifteen percent thickness ratio. Each airfoil has two plenum chambers which supply air to slots located beneath the leading and trailing edges, respectively. The rotor operates in cruise at advance ratios greater than unity so that the retreating blade is immersed in reverse flow. The lift and moments are controlled by ejecting a jet sheet out of the trailing edge on the advancing side of the azimuth and both the leading and trailing edge on the retreating side of the azimuth.

Standard blade element theory is used to calculate jet flap rotor performance thrust coefficients representative of actual full-scale rotor operation. It is shown that good performance can be obtained using the jet flap and that substantially better performance can be achieved using a circulation control airfoil.

DD FORM 1 NOV 68 1473 (PAGE 1)

S/N 0101-807-6801

UNCLASSIFIED

Security Classification

14. KEY WORDS	LINK A		LINK B		LINK C	
	ROLE	WT	ROLE	WT	ROLE	WT
Jet Flap Rotor						
Helicopter Performance						
3-D Wind Tunnel Testing						
High Advance Ratios						
Boundary Layer Control						

THEORETICAL PERFORMANCE OF A PURE JET FLAP ROTOR AT HIGH ADVANCE RATIOS

by

Robert M. Williams and Charles L. Bernitt

This work was performed under sponsorship of the Naval Air Systems Command (AIR-320).

December 1970 Technical Note AL-189

SUMMARY

The theoretical performance of a jet flap rotor at advance ratios greater than 1.0 is examined. The rotor is four-bladed with purely elliptical airfoils of fifteen percent thickness ratio. Each airfoil has two plenum chambers which supply air to slots located beneath the leading and trailing edges, respectively. The rotor operates in cruise at advance ratios greater than unity so that the retreating blade is immersed in reverse flow. The lift and moments are controlled by ejecting a jet sheet out of the trailing edge on the advancing side of the azimuth and both the leading and trailing edge on the retreating side of the azimuth.

Standard blade element theory is used to calculate jet flap rotor performance at thrust coefficients representative of an actual full-scale rotor operation. It is shown that good performance can be obtained using the jet flap and that substantially better performance can be achieved using a circulation control airfoil with tangential blowing over a rounded trailing edge.

Detailed calculations are presented for a model jet flap rotor to be wind tunnel tested at low thrust coefficients for validation with the above results.

TABLE OF CONTENTS

	Page
INTRODUCTION	1
THRUST COEFFICIENT RANGE	3
PERFORMANCE CALCULATION	3
EQUIVALENT LIFT-DRAG RATIO	4
MODEL ROTOR OPERATING CURVES	6
MODEL ROTOR TEST PROCEDURE	7
IMPROVEMENT OF PERFORMANCE	8
REFERENCES	10

LIST OF FIGURES

Figure 1 - Variation of Thrust Coefficient with Rotor Advance Ratio	11
Figure 2 - Thrust Coefficient Versus Disc Loading	12
Figure 3 - Equivalent Total Lift/Drag Ratio Versus Thrust Coefficient	13
Figure 4 - Equivalent Partial Lift/Drag Ratio Versus Thrust Coefficient	16
Figure 5 - Equivalent Total Lift/Drag Ratio Versus Rotor Advance Ratio	19
Figure 6 - Equivalent Partial Lift/Drag Ratio Versus Rotor Advance Ratio	21
Figure 7 - Total Shaft Torque Versus Total Rotor Thrust	23
Figure 8 - Shaft Horsepower Versus Thrust Coefficient	25
Figure 9 - Rotor RPM Versus Rotor Advance Ratio	27

Page

Figure 10 - Total Compressor Horsepower Versus Thrust Coefficient. 28

Figure 11 - Total Rotor Thrust Versus Advancing Blade Plenum Pressure 30

Figure 12 - Total Rotor Thrust Versus Retreating to Advancing Pressure Ratio 32

Figure 13 - Mass Flow Per Slot Versus Plenum Pressure . . . 34

Figure 14 - Total Rotor Mass Flow Versus Thrust Coefficient. 35

Figure 15 - Total Rotor Thrust Versus Thrust Coefficient. 37

Figure 16 - Comparison of Maximum Kinetic-Energy-Based Equivalent Lift-to-Drag Ratio for Three Configurations 39

LIST OF TABLES

Table 1 - Range of Variables for Proposed Test. 40

LIST OF SYMBOLS

A	slot area, 0.5192 in^2 (all blades)
C_d	section drag coefficient
C_T	rotor thrust coefficient, $\frac{T}{\pi R^2 (\Omega R)^2 \rho}$
C_μ	section momentum coefficient
d	section drag, lbs/ft
D_e	equivalent drag, $\frac{HP_s \times 550}{V_\infty} + D_r$, lbs
D_r	rotor drag, lbs
HP_c	total compressor horsepower required to supply the total mass flow in the rotor
HP_s	rotor shaft horsepower
HP_i	rotor induced horsepower
HP_p	rotor profile horsepower
L	total rotor lift, lbs
ℓ	section lift, lbs/ft
$(L/D_e)_T$	equivalent total lift to drag ratio
$(L/D_e)_p$	equivalent partial lift to drag ratio, i.e., not including rotor drag
M	advancing tip Mach number
M_∞	freestream Mach number
$\dot{m}_T$	total mass flow required through rotor, (lbs/sec)
$\dot{m}_s$	mass flow per slot, (lbs/sec)
N	rotor rpm
n	drive motor rpm

LIST OF SYMBOLS (continued)

P	rotor blade plenum pressure, lbs/in^2 absolute
P_A	rotor blade plenum pressure in the advancing sector of the rotor disk, lbs/in^2 absolute
P_R	rotor blade plenum pressure in the retreating sector of the rotor disk, lbs/in^2 absolute
P_T	rotor blade plenum pressure, lbs /in^2 absolute
Q_d	drive motor torque, in-lbs
Q_R	rotor torque, in-lbs
Q_s	total rotor shaft torque, in-lbs
R	rotor radius, ft
S	rotor disc area, ft^2
T	total rotor thrust, lbs
V_∞	tunnel freestream velocity, ft/sec
V_j	isentropic jet velocity, ft/sec
V_T	rotor tip velocity, ft/sec
μ	rotor advance ratio, V_∞/V_T
ρ	density of air, slugs/ft^3
Ω	rotor angular velocity, rad/sec
α	section angle of attack, degrees
ψ	azimuthal angle of rotor

INTRODUCTION

The feasibility of operating a helicopter rotor at advance ratios greater than 1.0 has been considered by several investigators. Tests have been run on very lightly loaded conventional rotors up to advance ratios of 1.45 (Reference 1) and shown to yield rotor equivalent lift-drag ratios as high as 13.0. Other investigators have proposed the use of bisymmetric airfoil sections on both rigid and flapping rotors to obtain high efficiencies. Unfortunately, conventional rotors operating at high advance ratios ($\mu > 1.0$) suffer from a myriad of dynamic and aeroelastic problems and incur severe design compromises to permit transistion through the intermediate advance ratio range ($0.5 \leq \mu \leq 1.0$). Furthermore, rotors generally increase greatly in both weight and complexity as the design advance ratio increases. These problems are brought about primarily by the dependence of the airfoil section lift on azimuthal velocity and angle of attack.

An alternative approach is to develop lift essentially independently of incidence and azimuthal velocity by using a method of circulation control such as suction or blowing. This report discusses the characteristic of a rotor with a blowing system called pure jet flap. The jet flap ejects a thin jet sheet from beneath the trailing edge and exhibits the characteristic that the lift coefficient varies essentially in proportion to the square root of the momentum coefficient. Therefore, by cyclically varying the blade duct pressure (hence the mass flow), the lift can be controlled to produce rotor forces and moments. A second feature of the jet flap is that most of the momentum flux used to create lift can be recovered as thrust and a final feature is the alleviation of many aeroelastic and dynamic constraints due to the removal of cyclic pitch hinges.

When applied to a rotor system operating at advance ratios greater than 1.0, the jet flap is utilized in both leading and trailing edge which are alternately blown depending on the direction of the relative wind.

Such a scheme was first proposed in a patent by Theodore von Karman and Yuan (Reference 2). Subsequently, a rotor model has been built and tested by the Lockheed Aircraft Corporation (Reference 3). The rotor was actually designed for use as a stoppable rotor concept, which when stopped, folded the blades back to a swept airplane-like configuration. The jet flap was incorporated primarily to provide control during the rotor stopping and starting phases of flight. These conditions corresponded to extremely high rotor disc loadings at very low tip speeds so that the thrust coefficients were as much as 100 times normal helicopter requirements. The results of the Lockheed tests showed that rotor controllability could be maintained but that rotor power was quite high.

The present study is an analytical extension of the jet flap rotor to low thrust coefficients where a high speed helicopter might operate. The study has been motivated by the availability of the Lockheed six-foot diameter jet flap rotor model and by separate studies of circulation control using tangential blowing on elliptical airfoils. These latter studies have indicated that extremely high rotor efficients are possible at advance ratios greater than 1.0. Although the jet flap rotor does not appear to be nearly as efficient as the circulation control rotor, it is nevertheless a worthwhile and convenient tool for investigating general blown rotor behavior at the high advance ratios ($\mu > 1$). The rotor will therefore be retested at low C_T/σ to demonstrate the high aerodynamic efficiencies predicted by theory.

THRUST COEFFICIENT RANGE

Figure 1 shows the variation of rotor thrust coefficient with advance ratio for a full scale rotor. Three disc loadings (T/S = 5, 10, 15) are shown and at each disc loading two cases are considered: (1) rotor slowing at a constant forward velocity of 300 ft/sec and, (2) rotor slowing at constant advancing tip Mach number of M = 0.806. The first case represents a more stringent requirement on the blade as it requires higher section lift coefficient on the retreating blade. The present study considers operation above $\mu = 1.0$ only.

To convert to a model scale with lower freestream and tip speeds, Figure 2 is used. For example, from Figure 1 for $\mu = 2.0$, T/S = 10 lb/ft^2 the value of C_T is 0.0465. Assuming a model test condition of 100 ft/sec rotor tip speed (200 ft/sec tunnel speed for $\mu = 2.0$) the corresponding disc loading is $T/S \approx 1.0$, or about 27 pounds of thrust on the six foot diameter model rotor.

PERFORMANCE CALCULATION

Standard rotor strip analysis was employed to calculate the low thrust coefficient rotor performance. Reference 1 describes a similar analysis in detail which successfully correlated the jet flap model rotor performance at very high thrust coefficient (maximum $C_T = 1.32$). In general, the agreement between theory and experiment was quite good. However, only compressor power was calculated as no section drag data was available.

The present analysis additionally includes computations of induced and profile power and also calculates the rotor in-plane drag. The section

drag data is calcuated from a curve fit of experimental data on a 15 percent jet flap, Reference 3. The approximate equation is:

$$C_d = 0.001\ \alpha^2 - 0.005\ \alpha + 0.015 - 0.8\ C_\mu$$

The last term in this equation indicates that 80 percent of the jet momentum flux was recovered as thrust. It should be noted that the design jet exit angle of the model was 30 degrees as opposed to the rotor section design exit angle of 40 degrees. The latter also appeared to have encountered some upper surface separation near the trailing edge which may have caused a large reduction in thrust recovery. The simultaneous blowing on the retreating blade was assumed to have no effect on drag although it can be shown that ideally most of the leading edge momentum flux will be recovered as thrust, despite the jet issuing forward. These considerations caused some doubt as to the validity of the drag equation, but it is felt that it still gives approximate characteristics.

The rotor in-plane drag was computed using the standard rotor assumption of zero spanwise velocity. This would tend to underestimate the rotor drag force at the very high advance ratios considered.

EQUIVALENT LIFT-DRAG RATIO

The resultant power and rotor drag calculation (all at zero shaft angle) were then expressed as an equivalent lift-drag ratio. This parameter is a direct indication of efficiency of a lifting system where the equivalent drag is given by:

$$D_e = (HP_c + HP_p + HP_i) \times 550/V_\infty + D_r$$

Both partial (based only on $HP_i + HP_p + HP_c$), and total (all terms) equivalent lift-drag ratios have been calculated for two freestream velocities for the six foot model rotor described in Reference 3. The dimensionless results are, of course, equally valid for a full-scale rotor.

The variation of total equivalent rotor lift-drag ratio is shown in Figure 3. It may be seen that an optimum L/D_e exists at the low thrust coefficient and that this value also increases with advance ratio. It can also be noted that the curves for V_∞ = 130 and 200 feet per second are identical, Figures 3 (a) and 3 (b). This is due primarily to the incompressible Mach number range in which the model rotor operates. At high advancing tip Mach numbers some degradation in performance would be expected although this could be offset substantially by the favorable high Mach number behavior of a jet flap.

Figure 3 (c) presents the rotor behavior at 200 ft/sec for various levels of model rotor thrust. The rapid increase in L/D_e with μ shows that even this relatively crude high advance ratio blown rotor would be capable of good performance. As advance ratio increases further the rotor essentially approaches a high aspect ratio wing with its inherent high efficiency.

Figure 4 presents the variation of partial equivalent lift-drag ratio (in-plane drag not included). In general, these values are approximately twice those of the total L/D_e so that any reduction of in-plane drag would produce a sufficient performance improvement. Of additional interest, Figure 4 (a), is the autorotative region where the rotor develops zero or negative shaft torque. Due to the extreme sensitivity of the autorotation mode to section profile drag and shaft angle, this region should be regarded as tentative only. Although the present results indicate

that such operation may not be economical, it should be studied further before drawing a final conclusion. In actual practice it may be possible to select the solidity, shaft angle and section characteristics such that the full-scale rotor can autorotate at the design condition.

Figures 5 and 6 present cross plots of the previous data to show the variation of L/D_e with advance ratio for constant model thrust. The variation of efficiency at constant thrust by varying freestream velocity can be noted from these curves.

MODEL ROTOR OPERATING CURVES

The remaining curves are presented as a guide to the model rotor behavior and for determining the drive system and instrumentation requirements. The data presented here has been computed for advance ratios up to 2.0 and zero shaft angle. Additional investigations of higher advance ratios and positive (rearward) shaft angles would be of interest also.

Figures 7 and 8 show the variation of shaft torque and shaft power up to a C_T of 0.10. It can be noted that the rotor will autorotate at 130 ft/sec but not at 200 ft/sec. The relation between drive motor torque and rotor torque is:

$$Q_d = \frac{N}{n} Q_R$$

Using the working curves of Figure 9 the drive motor and pulley ratio can be determined.

Figure 10 shows the variation in the adiabatic compressor power (or alternatively kinetic energy flux of the jet). In general, for the jet flap rotor this term dominates the partial equivalent lift drag ratio. It is approximately equal in magnitude to the rotor in-plane power.

Figures 11 and 12 show the variation of rotor thrust for various advancing blade pressures and for retreating to advancing blade pressure ratio.

These values are determined for a rotor roll trim condition with the advancing blade slot generally unchoked and the retreating blade choked.

Figures 13 and 14 show the mass flow variation with blade pressure and thrust coefficient, respectively.

Figure 15 is a working curve for use in interpreting the previous data.

MODEL ROTOR TEST PROCEDURE

Each data point taken while running the wind-tunnel test will be for a set freestream velocity, rotor advance ratio and rotor thrust coefficient. The procedure for setting these test conditions requires a manual reading and/or adjustment of freestream velocity, rotor RPM, advancing and retreating blade plenum pressure, and rotor roll force. In general, the tunnel operators will (1) bring the rotor RPM up to the value corresponding to the rotor advance ratio desired, (2) set the freestream tunnel velocity, (3) set the advancing blade pressure to the prescribed value in order to set approximately the desired thrust coefficient, and (4) adjust the retreating blade pressure for zero roll force. The pressure adjustment must be made while holding a constant rpm. The procedure will be repeated through a range of thrust coefficients, advance ratios and freestream velocity, in that order. The following table shows the range of test variables needed to verify the analysis in this report. It is recommended that a range of shaft inclination angles also be run.

IMPROVEMENT OF PERFORMANCE

The overall rotor aerodynamic performance for any given flight condition is primarily dependent on two factors, (1) the airfoil section characteristics, and (2) the azimuthal loading (blowing) distribution. It is also dependent to a lesser degree on slot distribution, solidity, planform and twist.

The airfoil section characteristics can be greatly improved by the use of tangential blowing rather than pure jet flap blowing. Figure 16 shows a comparison of maximum section equivalent lift-drag ratios for three 15 percent ellipses from Reference 4. The "Rounded Ellipse" and "Pure Ellipse" have tangential blowing while the "Jet Flap" is a pure jet flap exiting at a 30 degree angle beneath the chord line. It can be seen that very large improvements in efficiency are possible using the tangential blowing method.

The azimuthal loading can also be greatly improved by changing the present square wave pressure input to a harmonic input of the form:

$$P_T = P_T(1 + a_1 \sin \psi + b_1 \cos \psi + a_2 \sin^2 \psi + b_2 \cos^2 \psi + \ldots).$$

The simultaneous leading and trailing edge blowing on the retreating side of the azimuth should be removed. These two changes will greatly reduce compressor power requirements.

The effect of rotor attitude has not been investigated in the present study. However, similar studies of circulation control rotors indicate that significant increases in rotor L/D_e are possible with approximately five degrees of rearward inclination. In this case the rotor can operate in a near autorotative mode.

Aviation and Surface Effects Department
Naval Ship Research and Development Center
Washington, D. C. 20034
December 1970

ACKNOWLEDGEMENT

The authors would like to acknowledge the assistance of Mr. John Di Joseph for conducting some of the early performance correlations and Dr. Ettore Mori for developing the rotor performance program.

REFERENCES

1. Jenkins, Julian L., Jr. Wind-Tunnel Investigation of a Lifting Rotor Operating at Tip-Speed Ratios From 0.65 to 1.45. Wash., Feb 1965. 20 p. incl. illus. (National Aeronautics and Space Adm. Tech. Note D-2628).

2. Yuan, Shao Wen and Theodore von Karman. Lift Rotor Control. [Wash.] 21 Aug 1956 (Patent Office. 2,759,548).

3. Kuczynski, W. A. and K. B. Lewis. Jet Flap Cyclic Twist Feasibility Research Program. Burbank, Mar 1970. 157 p. incl. illus. (Lockheed-California Co. LR 22973. Contract N00019-68-C-0285).

4. Englar, Robert J. Two-Dimensional Transonic Wind Tunnel Tests of Three 15 Percent Thick Circulation Control Airfoils. Wash., Dec 1970. 63 l. incl. illus. (Naval Ship Research and Development Center. Tech Note AL-182).

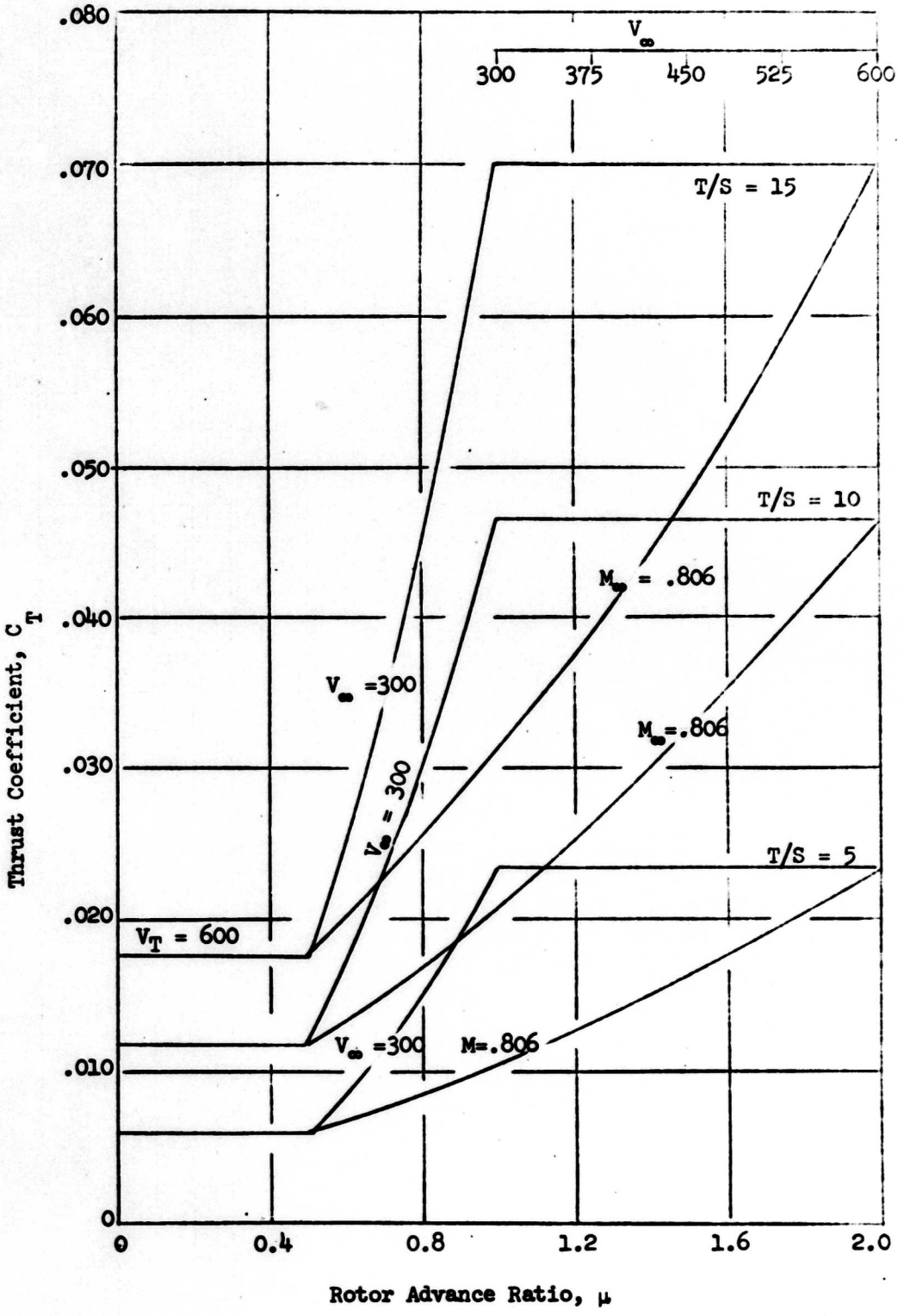

Figure 1 - Variation of Thrust Coefficient with Rotor Advance Ratio

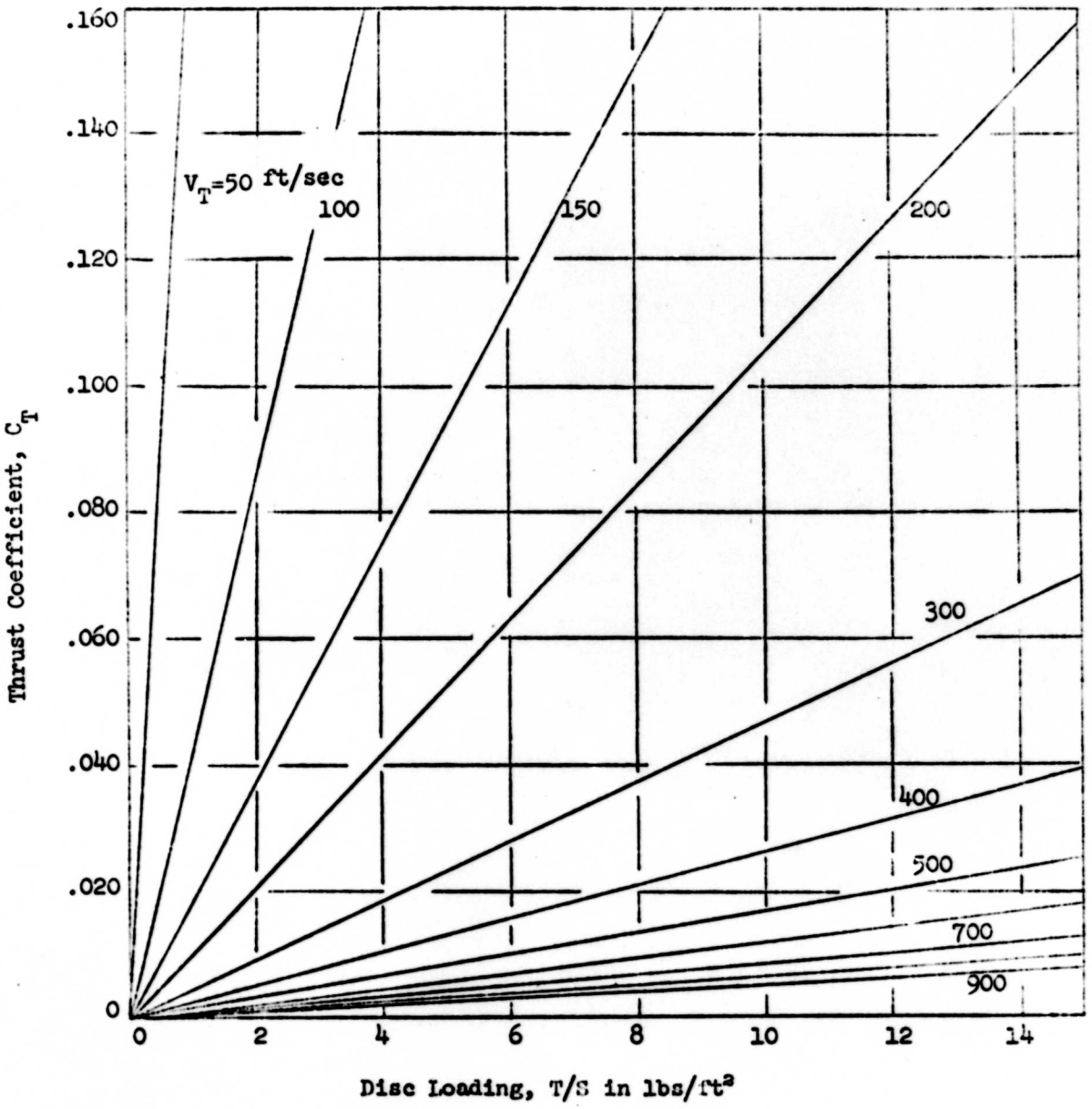

Figure 2 - Thrust Coefficient Versus Disc Loading

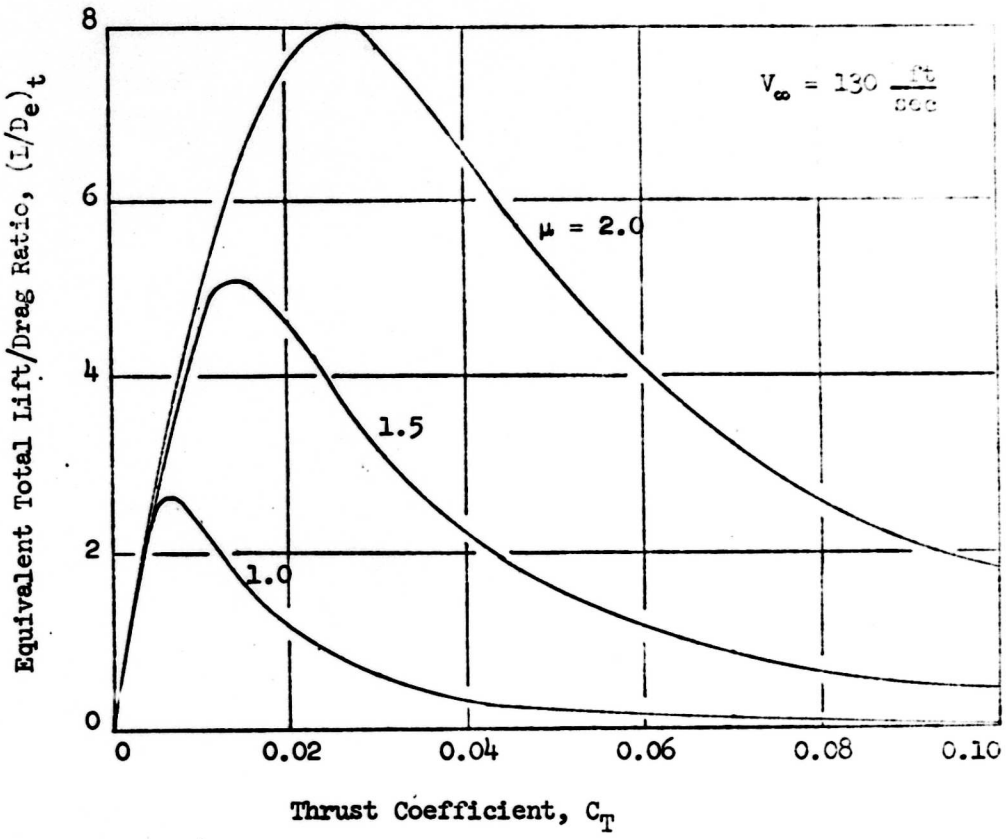

Figure 3 - Equivalent Total Lift/Drag Ratio Versus Thrust Coefficient

(a) V_∞ = 130 ft/sec

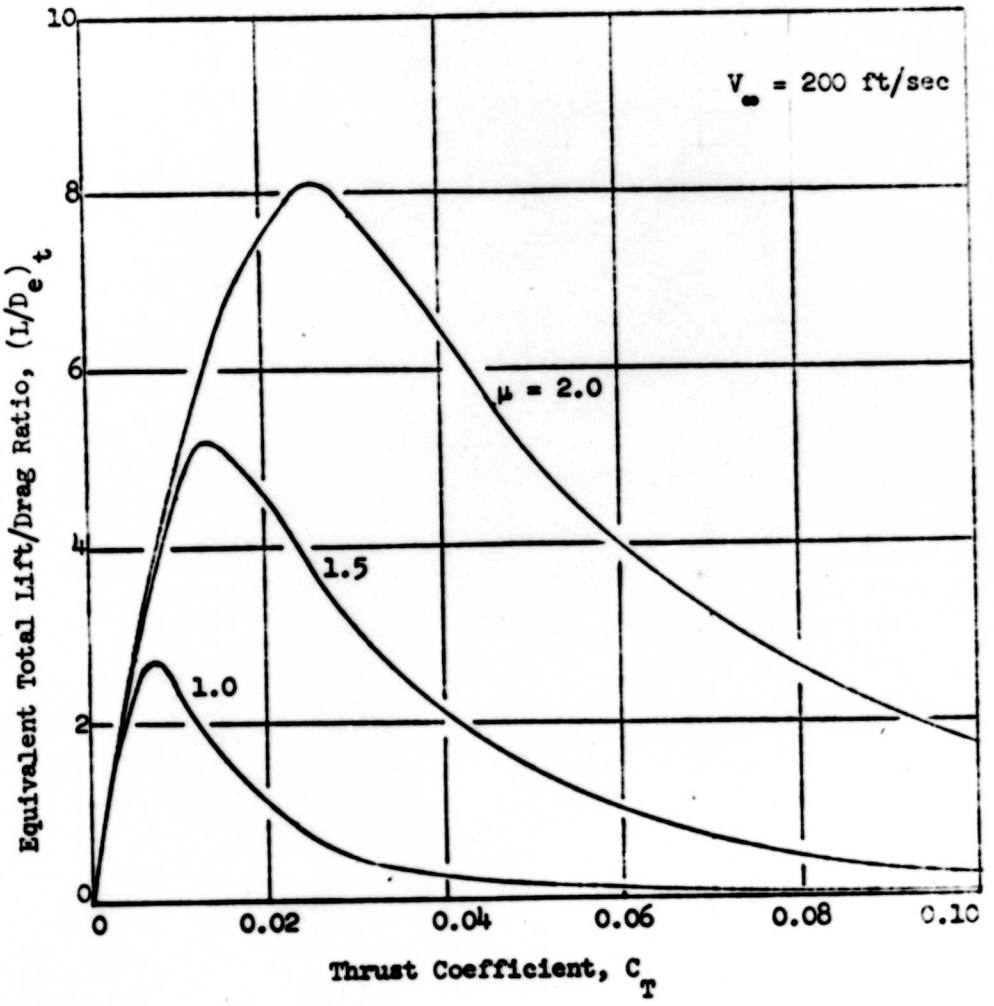

Figure 3 - (continued)

(b) V_∞ = 200 ft/sec

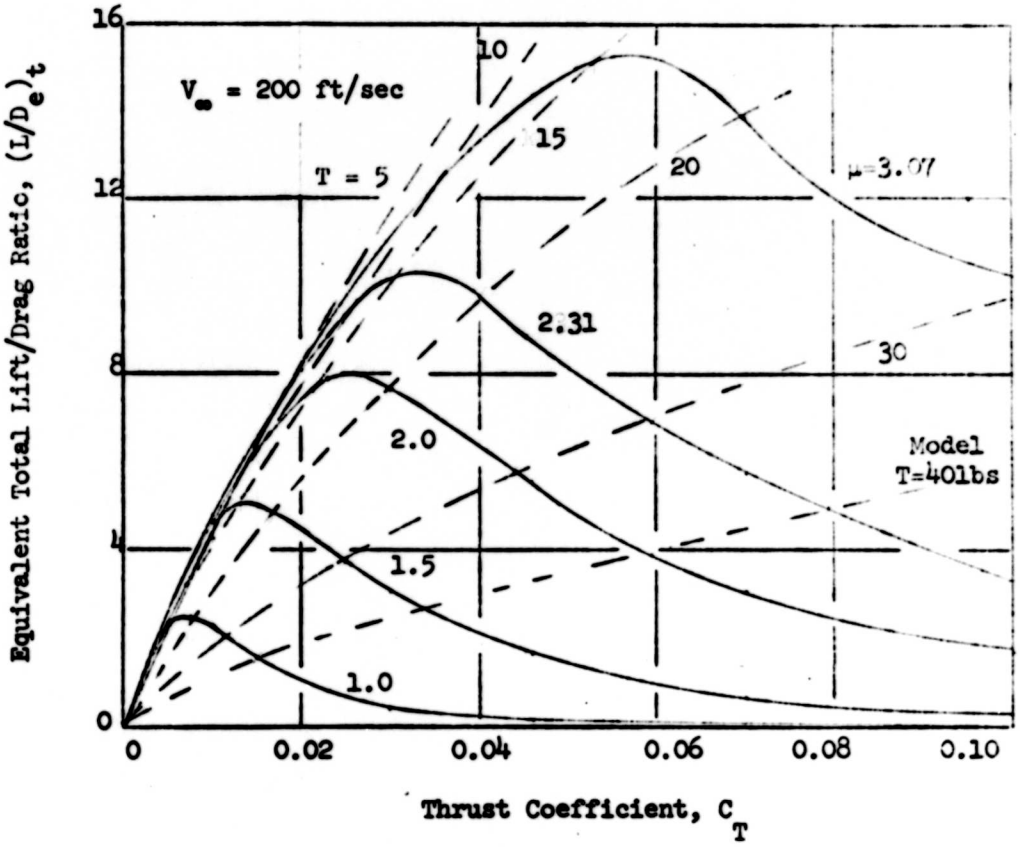

Figure 3 - (concluded)

(c) V_∞ = 200 ft/sec, High Advance Ratio

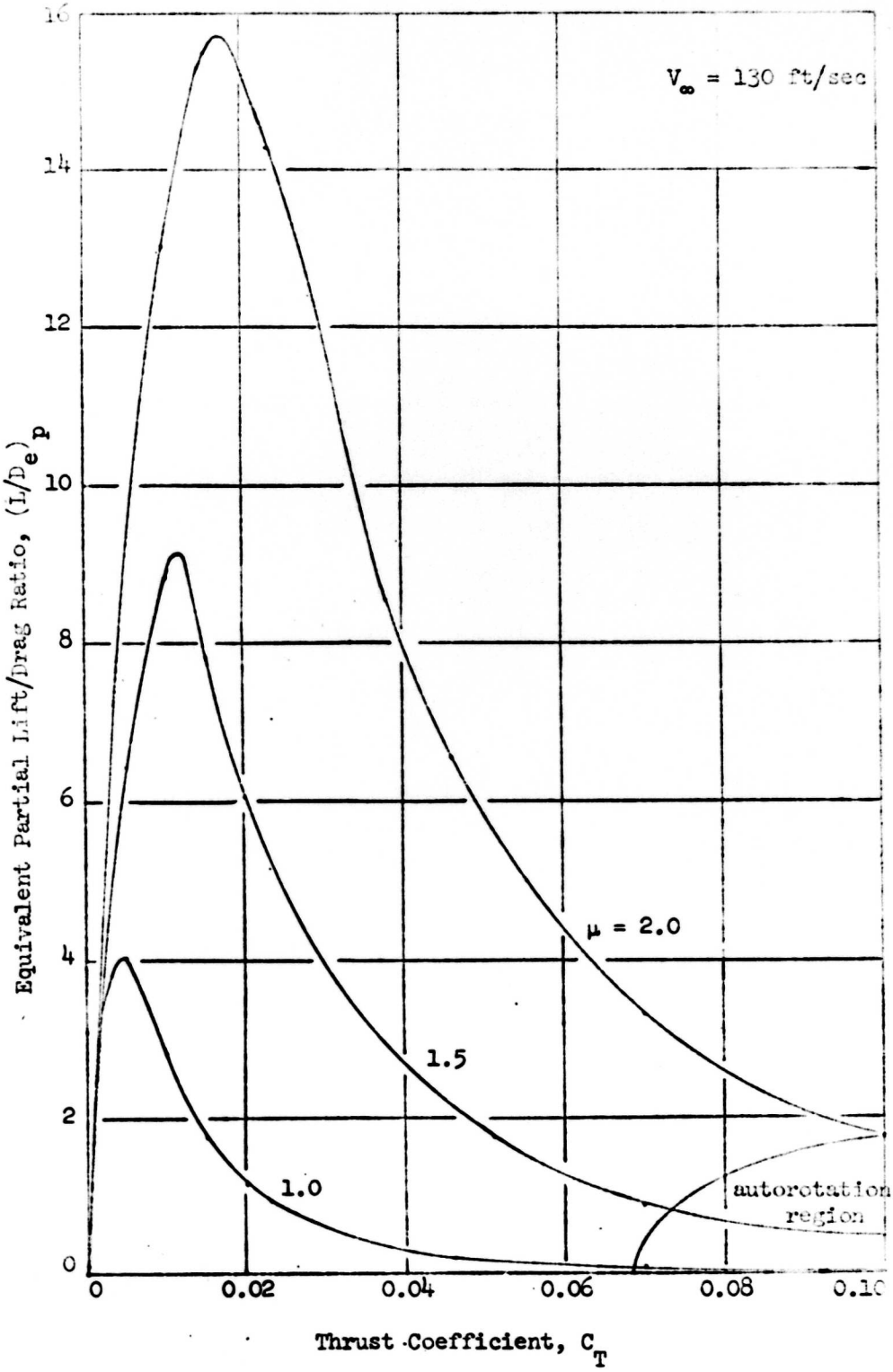

Figure 4 - Equivalent Partial Lift/Drag Ratio Versus Thrust Coefficient

(a) V_∞ = 130 ft/sec

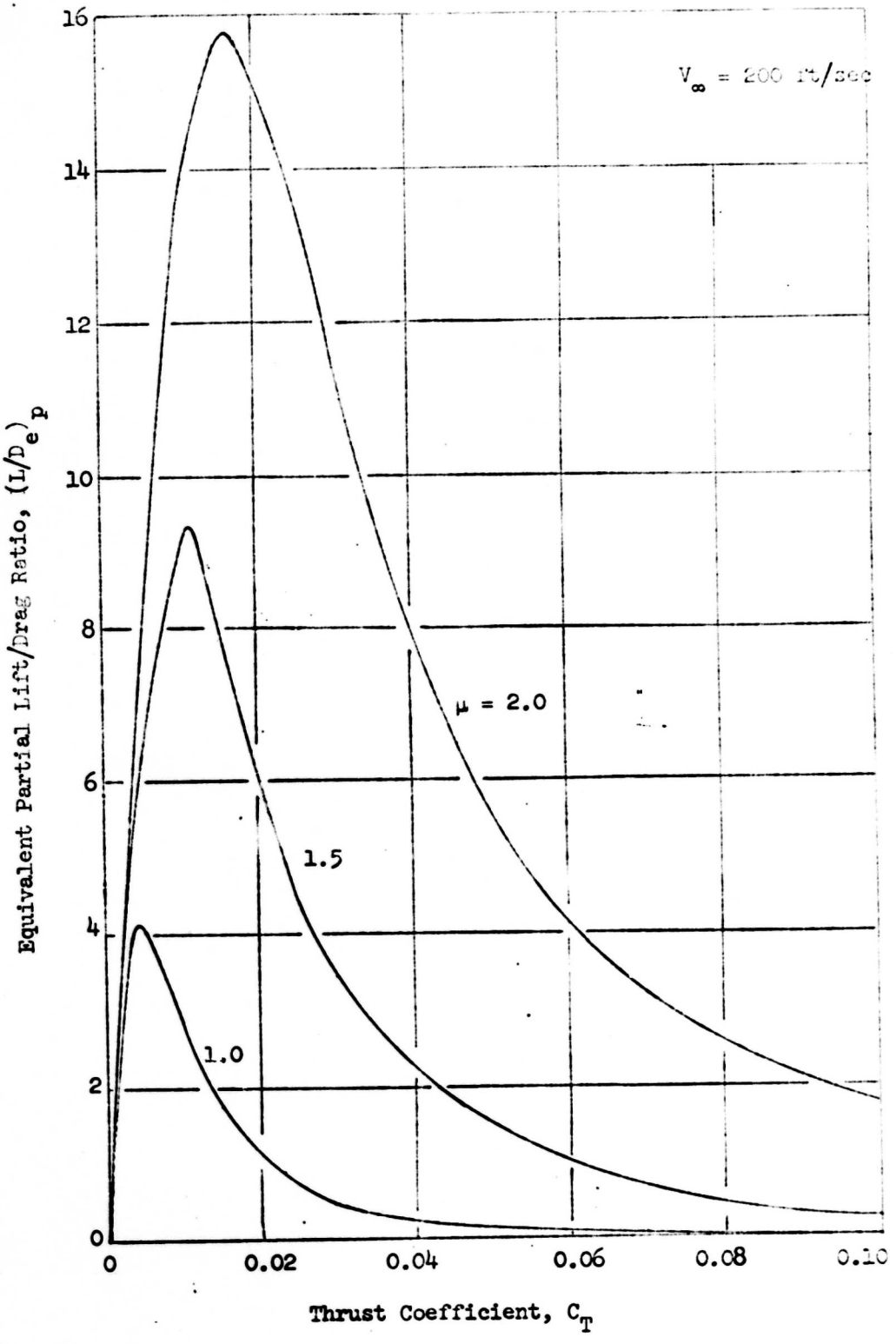

Figure 4 - (Continued)

(b) V_∞ = 200 ft/sec

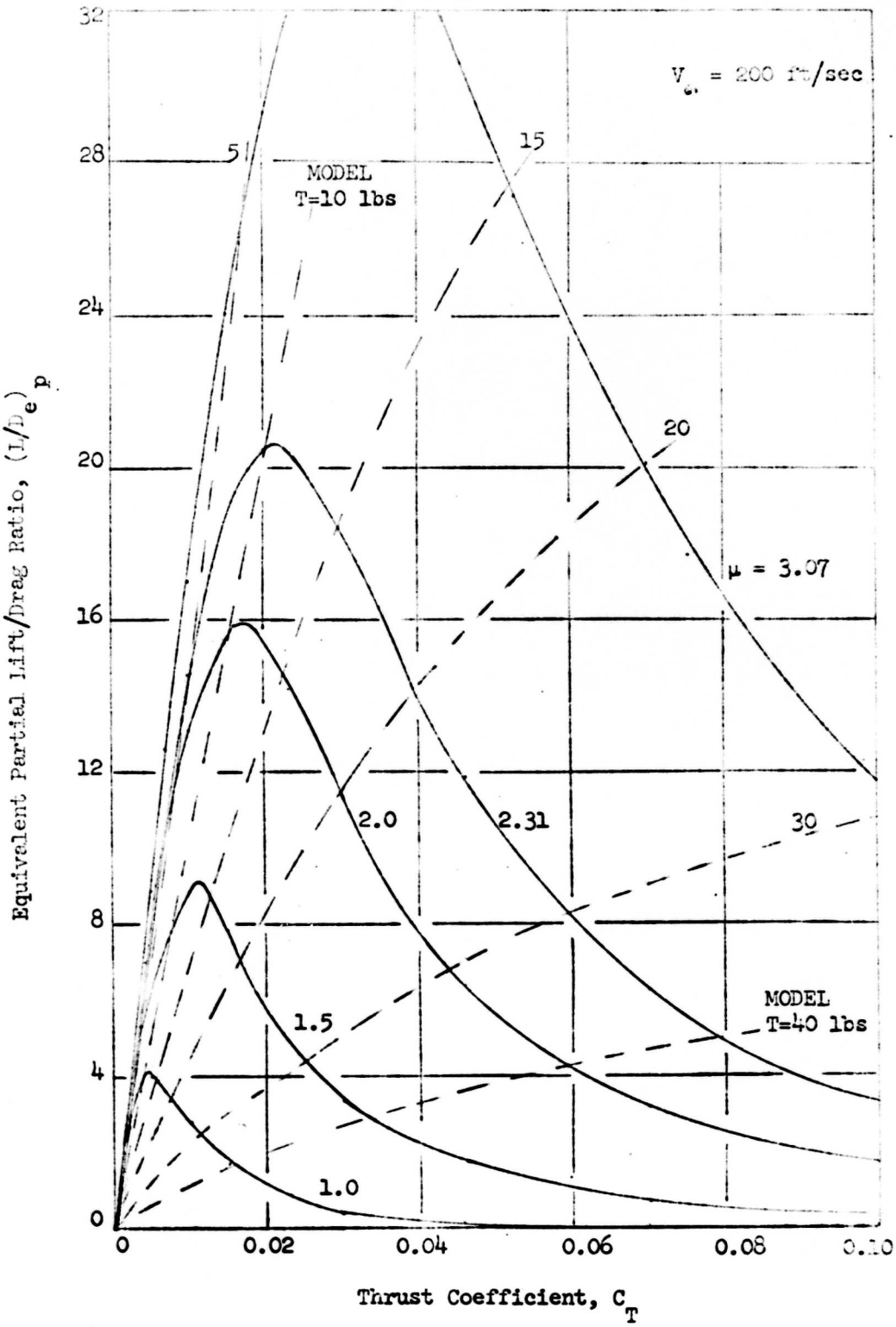

Figure 4 - (Concluded)

(c) V_∞ = 200 ft/sec, high advance ratio

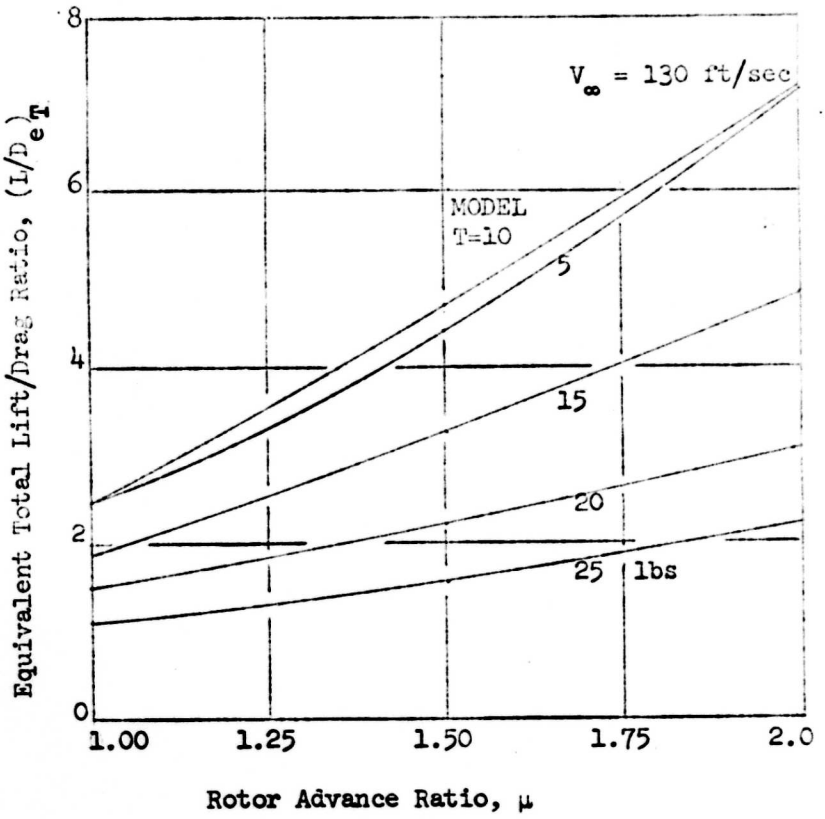

Figure 5 - Equivalent Total Lift/Drag Ratio Versus Rotor Advance Ratio

(a) V_∞ = 130 ft/sec

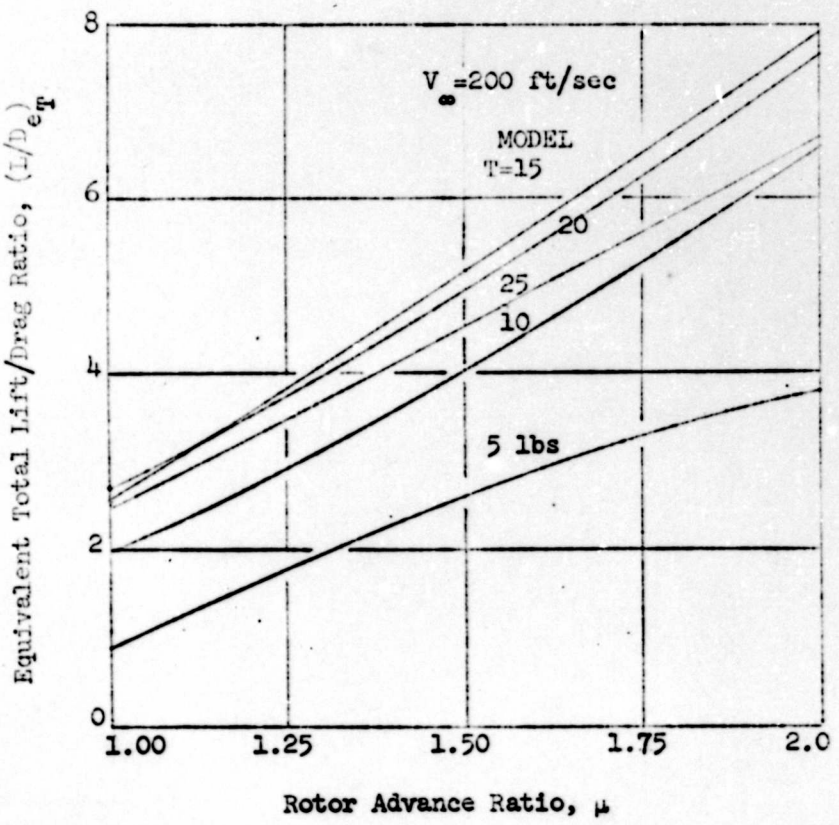

Figure 5 - (concluded)

(b) V_∞ = 200 ft/sec

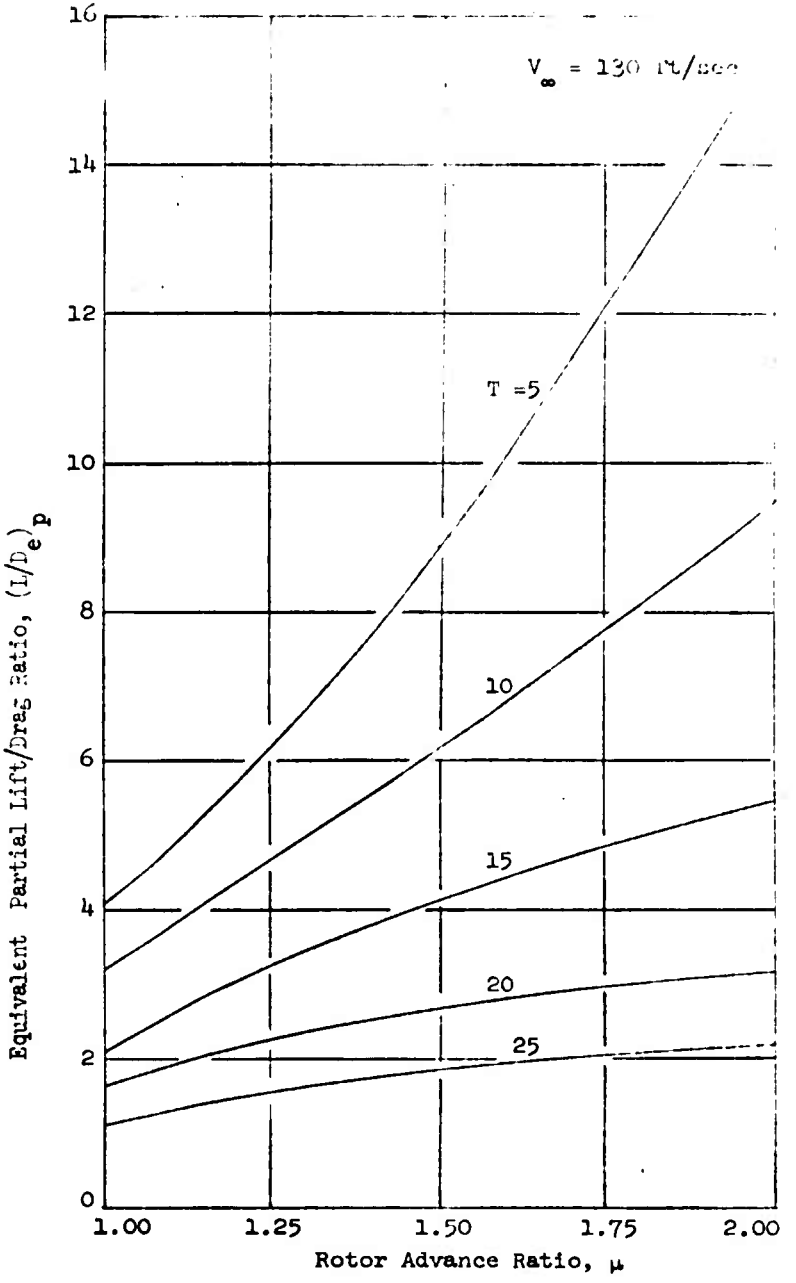

Figure 6 - Equivalent Partial Lift/Drag Ratio Versus Rotor Advance Ratio

(a) V_∞ = 130 ft/sec

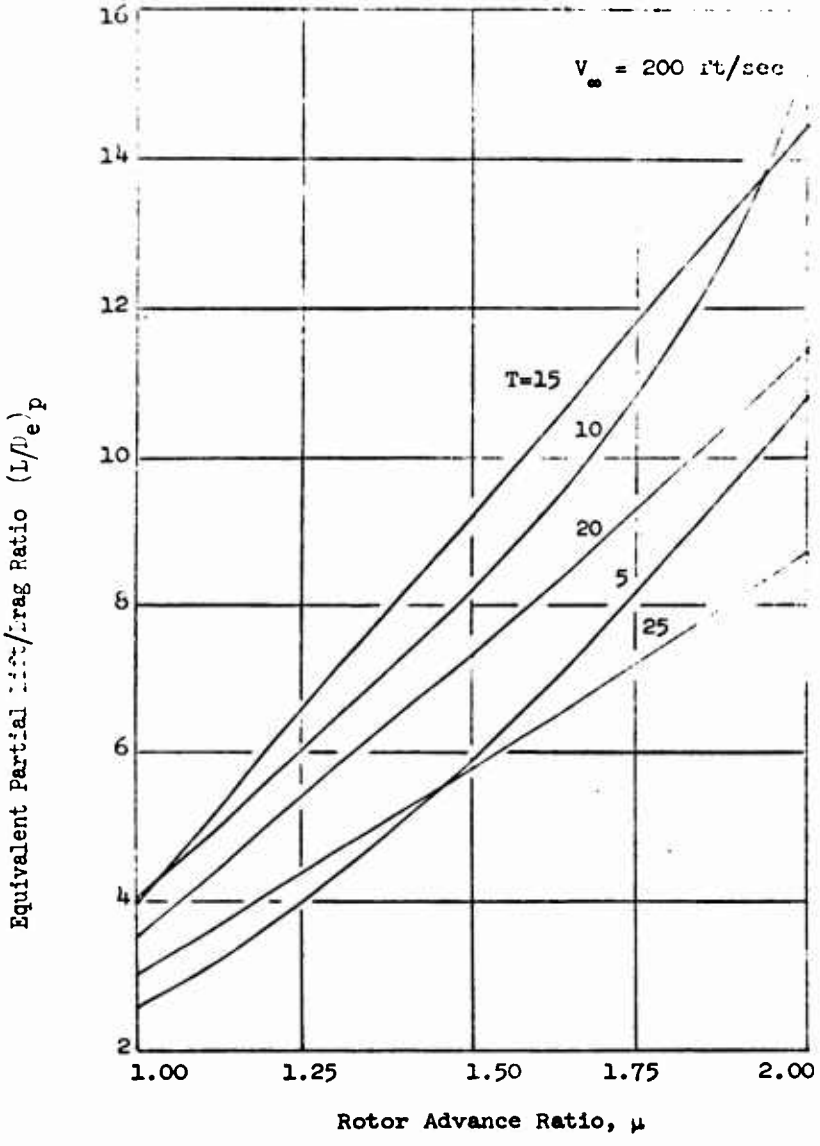

Figure 6 - (concluded)

(b) V_∞ = 200 ft/sec

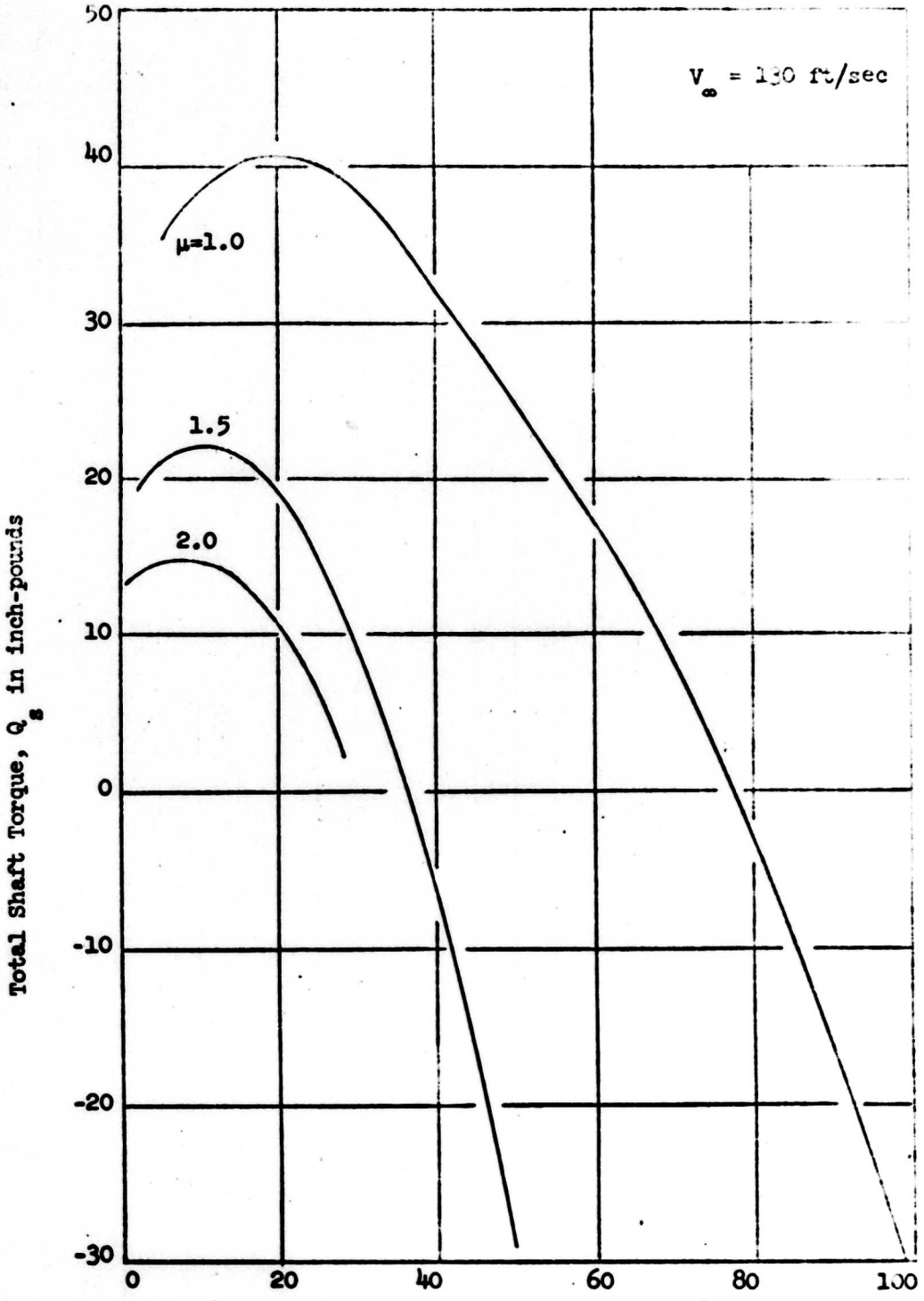

Figure 7 - Total Shaft Torque Versus Total Rotor Thrust

(a) V_∞ = 130 ft/sec

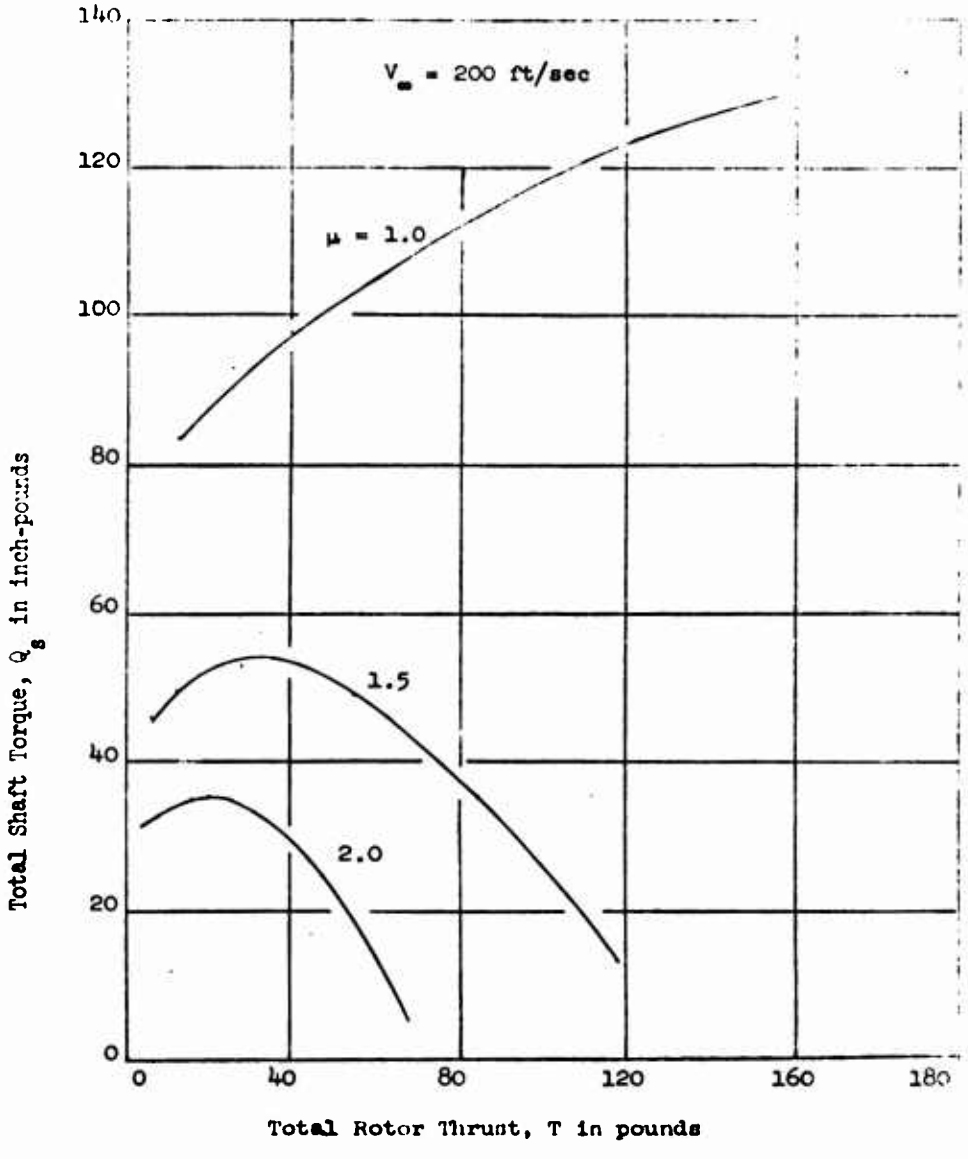

Figure 7 - (Concluded)

(b) V_∞ = 200 ft/sec

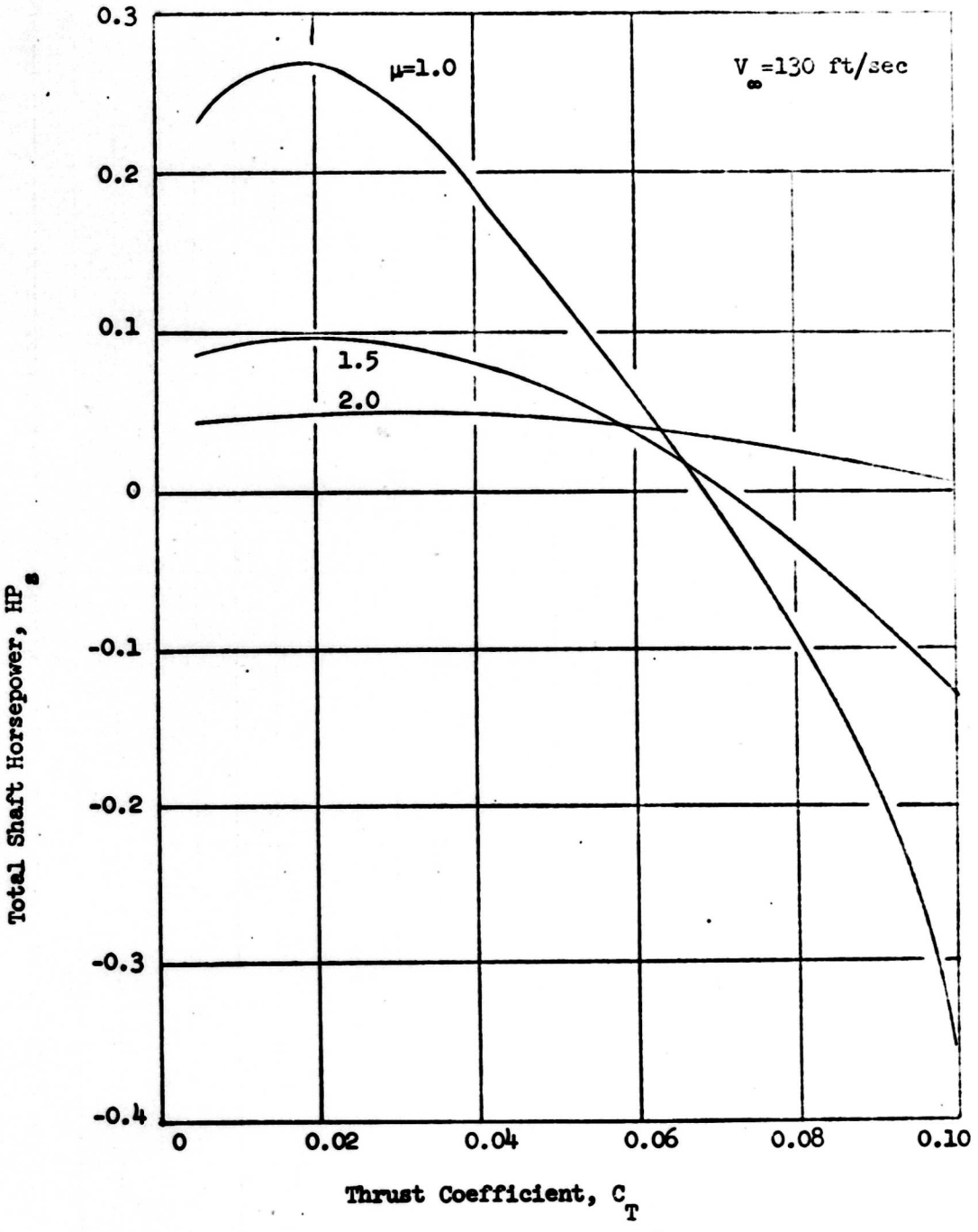

Figure 8 - Shaft Horsepower Versus Thrust Coefficient

(a) V_∞ = 130 ft/sec

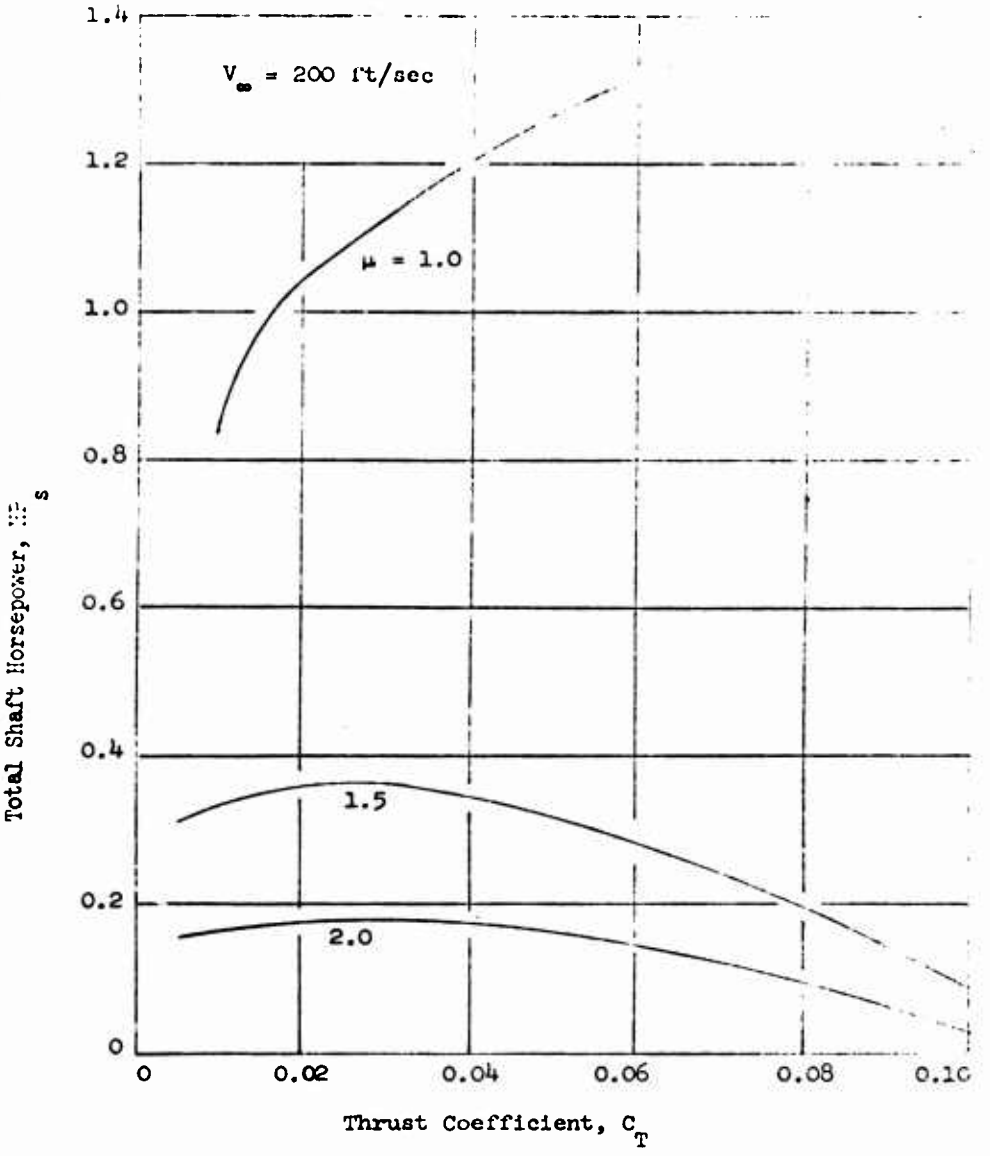

Figure 8 - (Concluded)

(b) V_∞ = 200 ft/sec

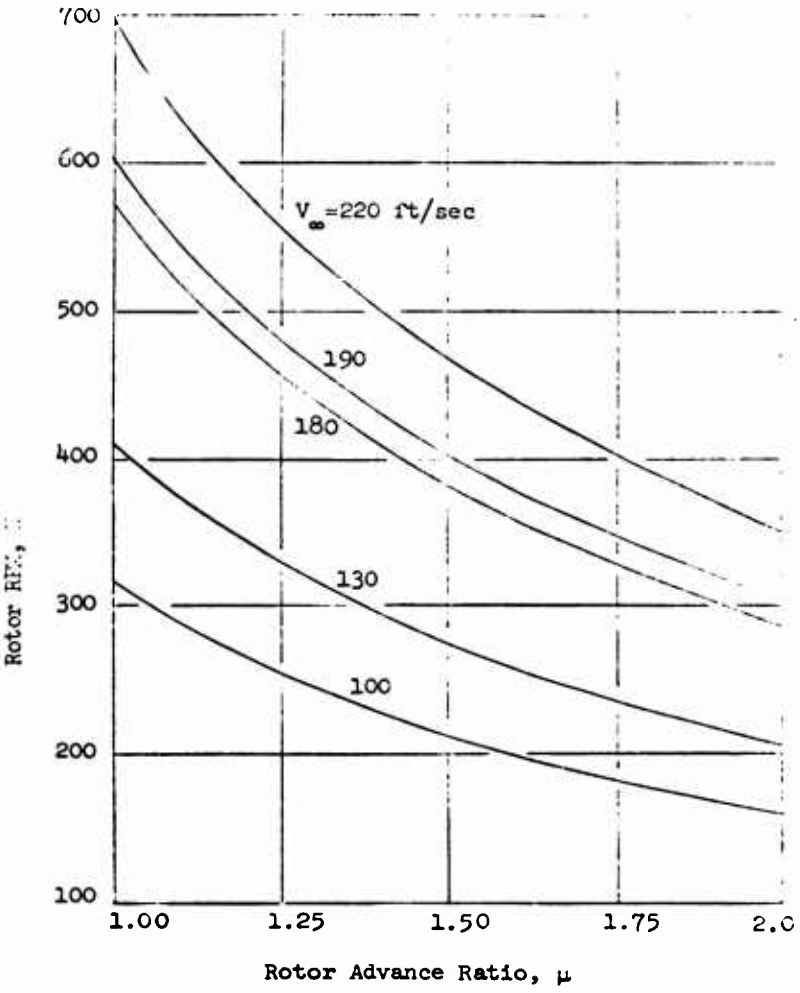

Figure 9 - Rotor RPM Versus Rotor Advance Ratio

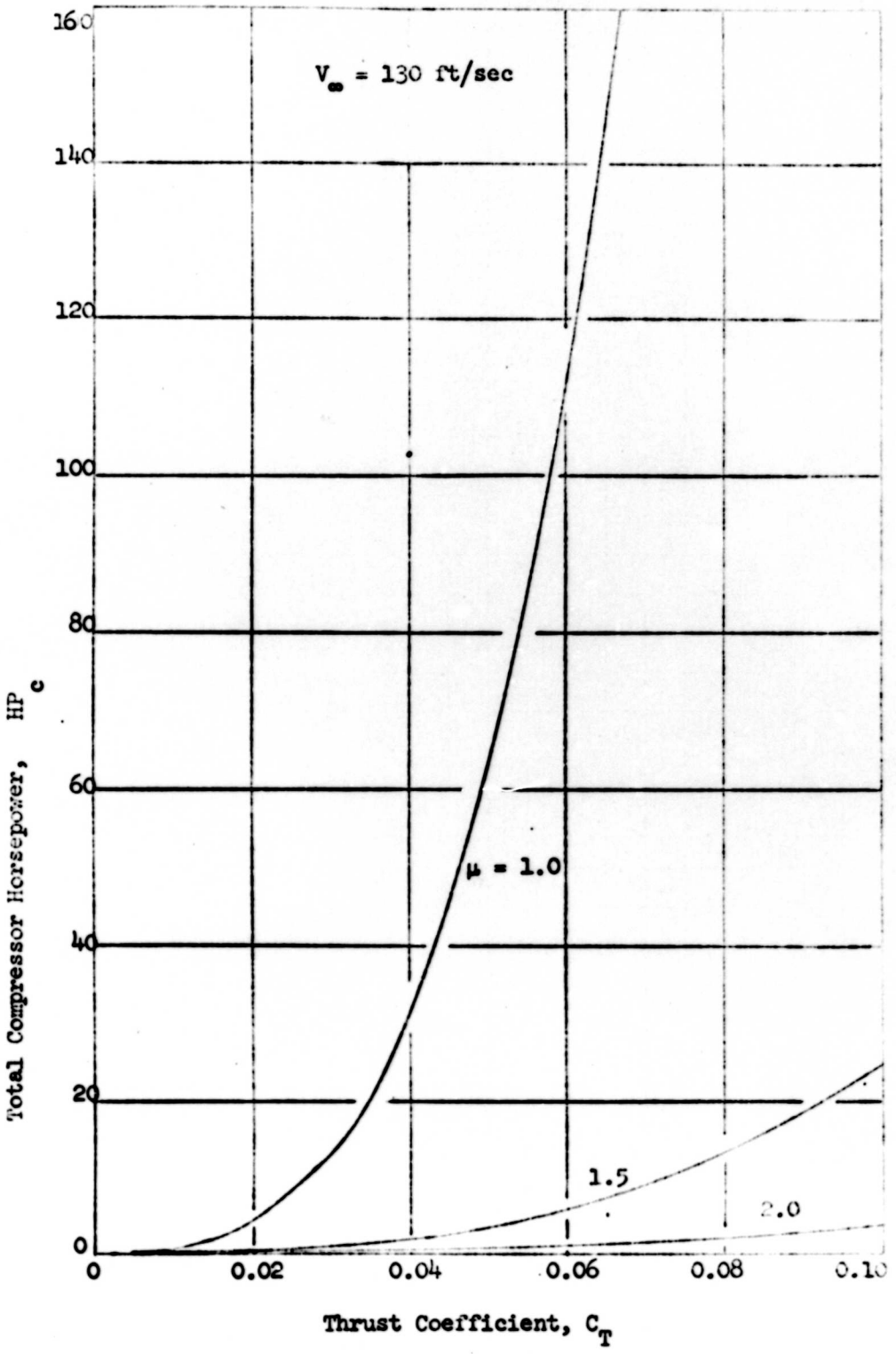

Figure 10 - Total Compressor Horsepower Versus Thrust Coefficient

(a) V_∞ = 130 ft/sec

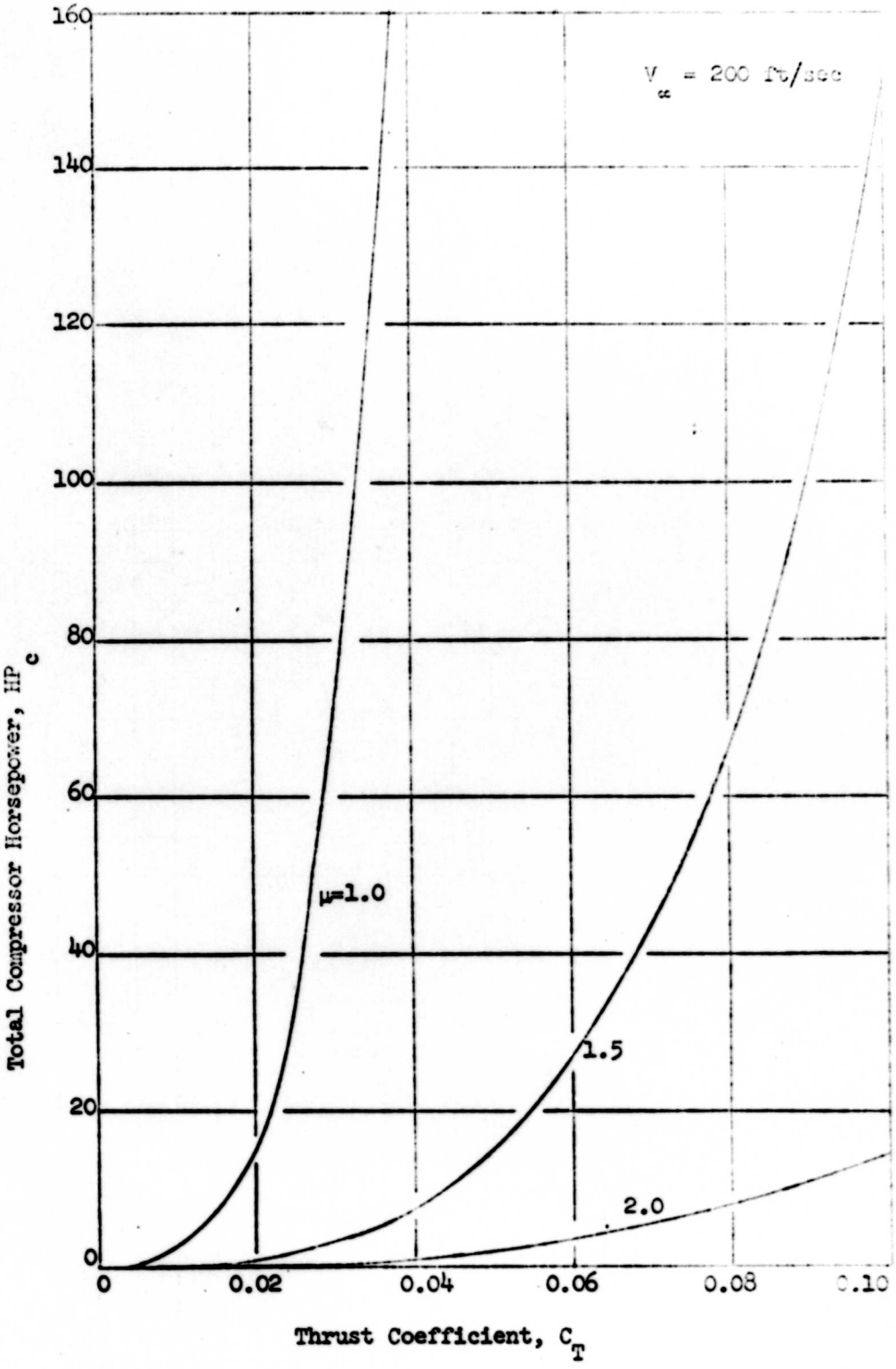

Figure 10 - (Concluded)

(b) V_∞ = 200 ft/sec

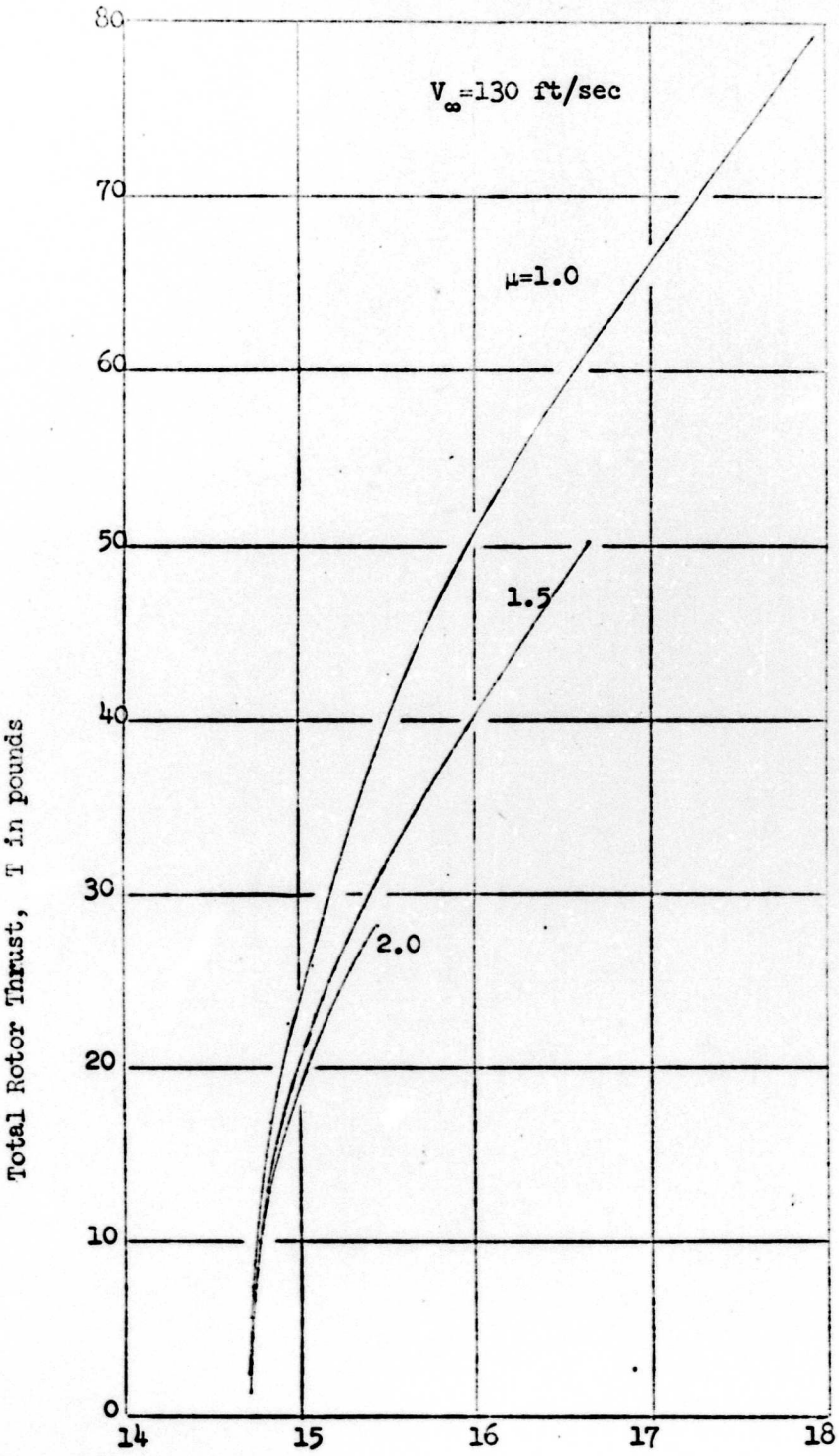

Figure 11 - Total Rotor Thrust Versus Advancing Blade Plenum Pressure

(a) V_∞ = 130 ft/sec

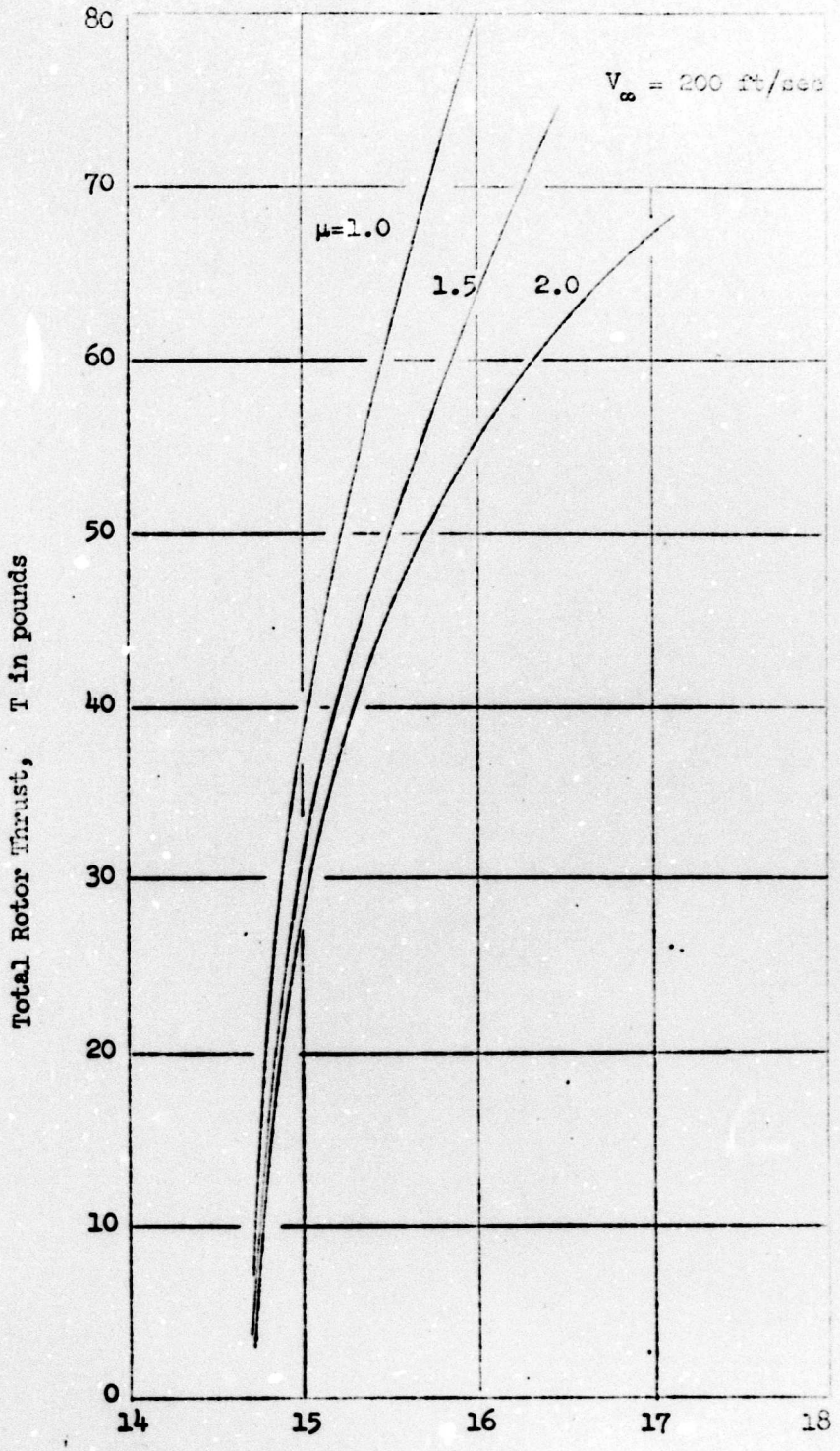

Figure 11 - (Concluded)

(b) V_∞ = 200 ft/sec

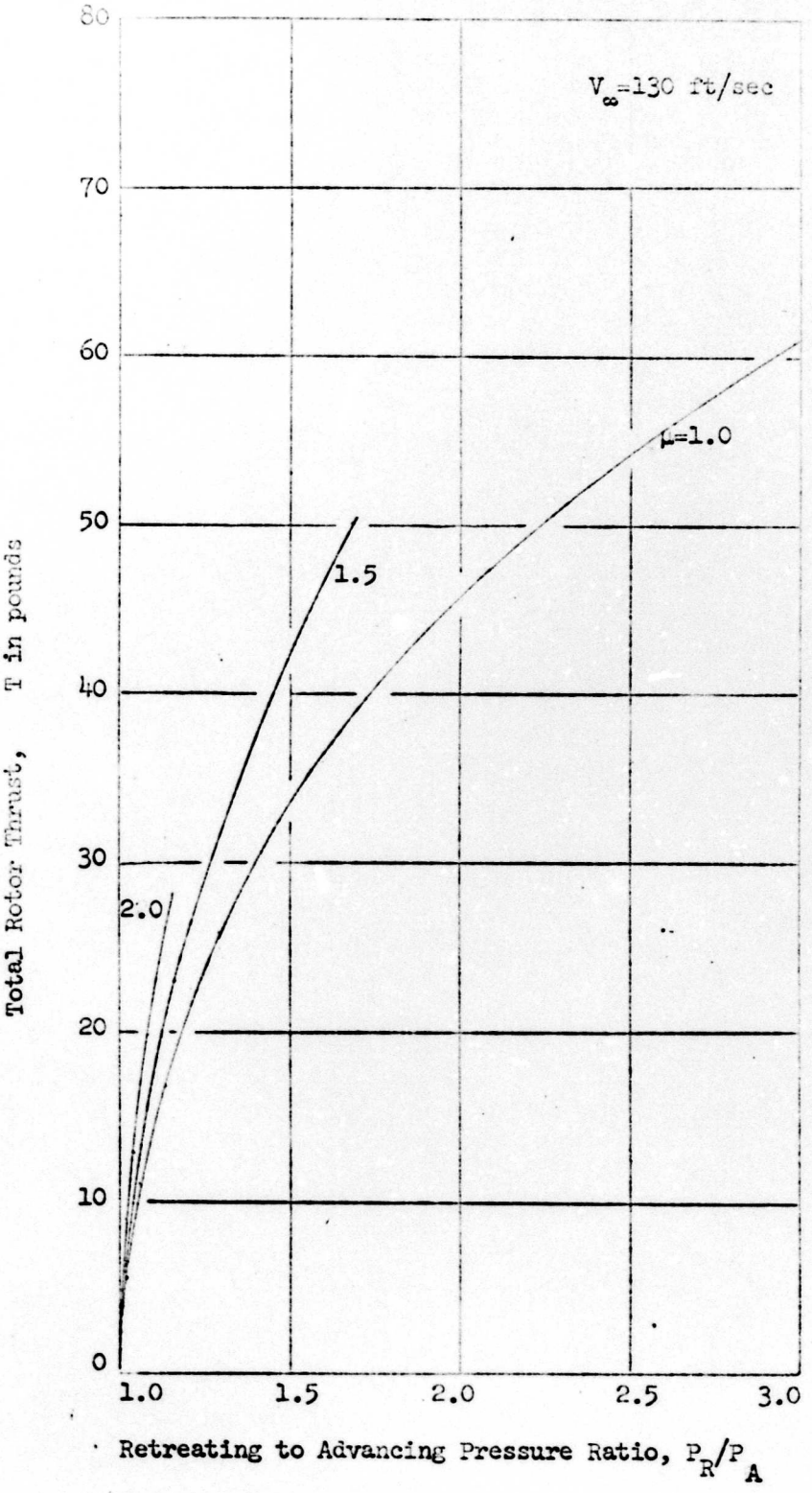

Figure 12 - Total Rotor Thrust Versus Retreating to Advancing Pressure Ratio

(a) V_∞ = 130 ft/sec

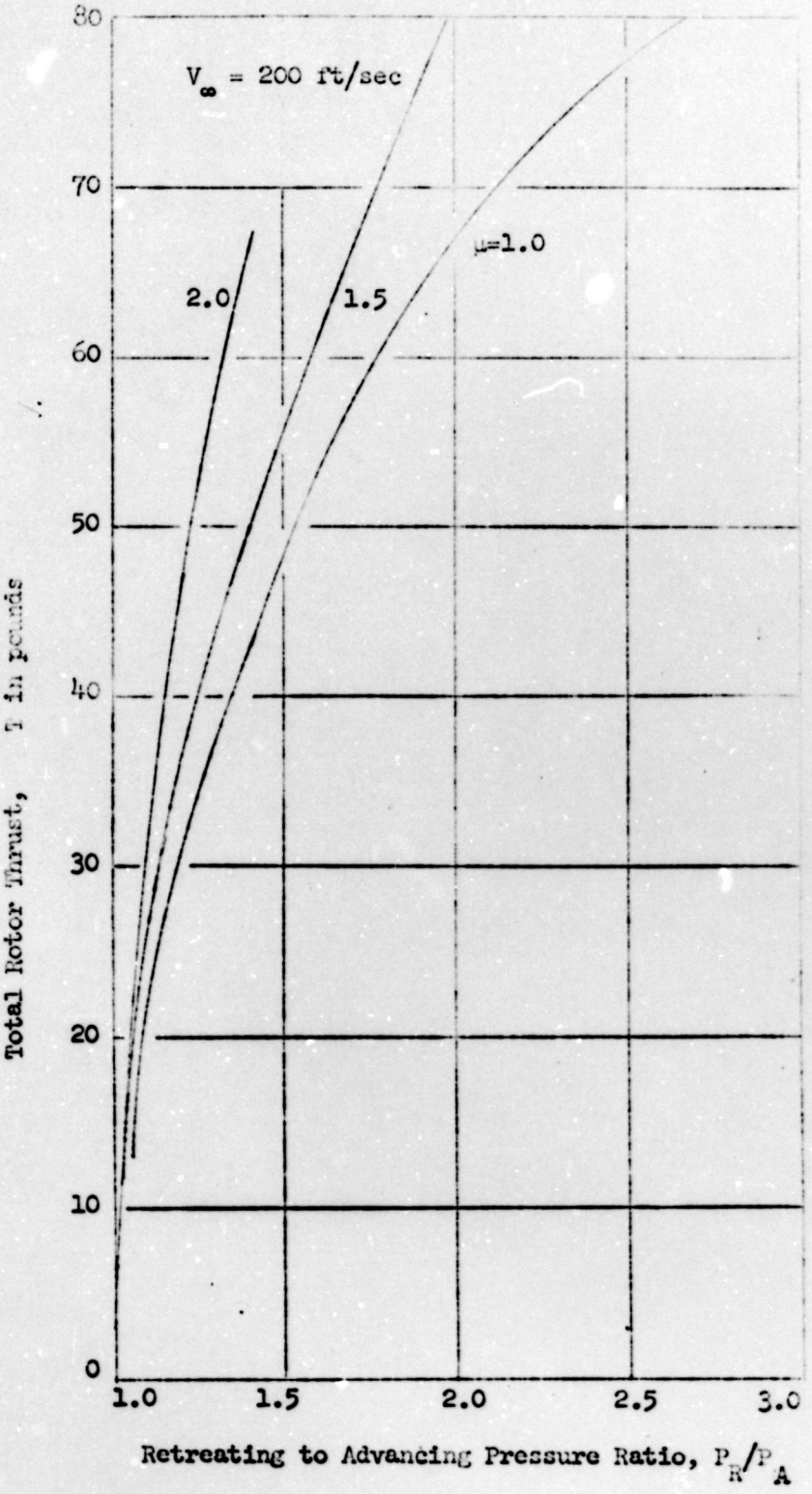

Figure 12 - (Concluded)

(b) V_∞ = 200 ft/sec

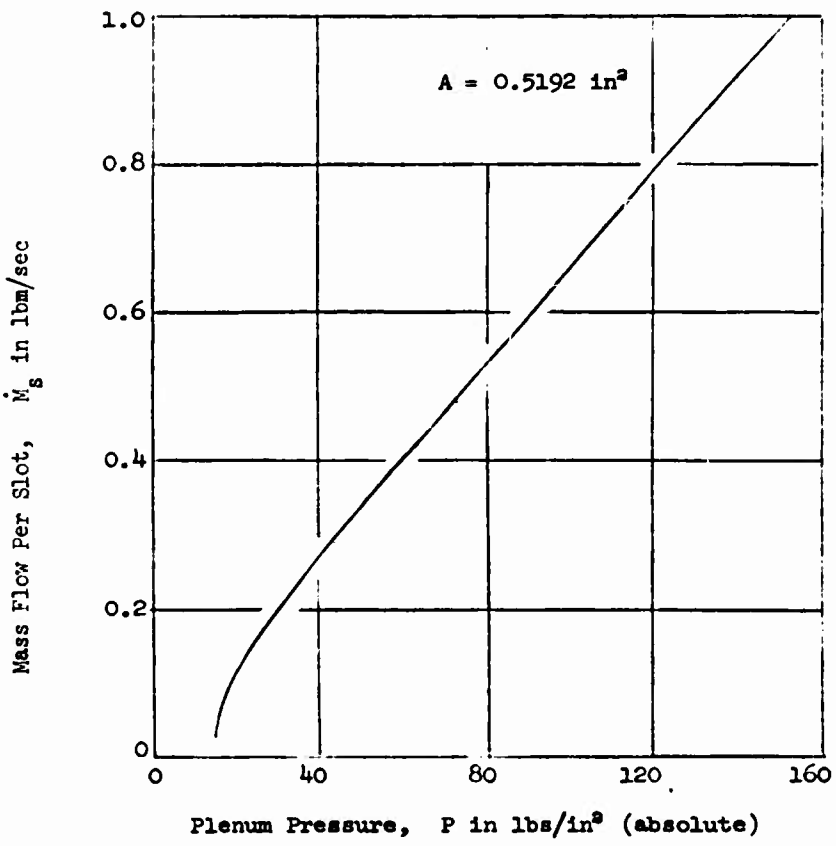

Figure 13 - Mass Flow Per Slot Versus Plenum Pressure

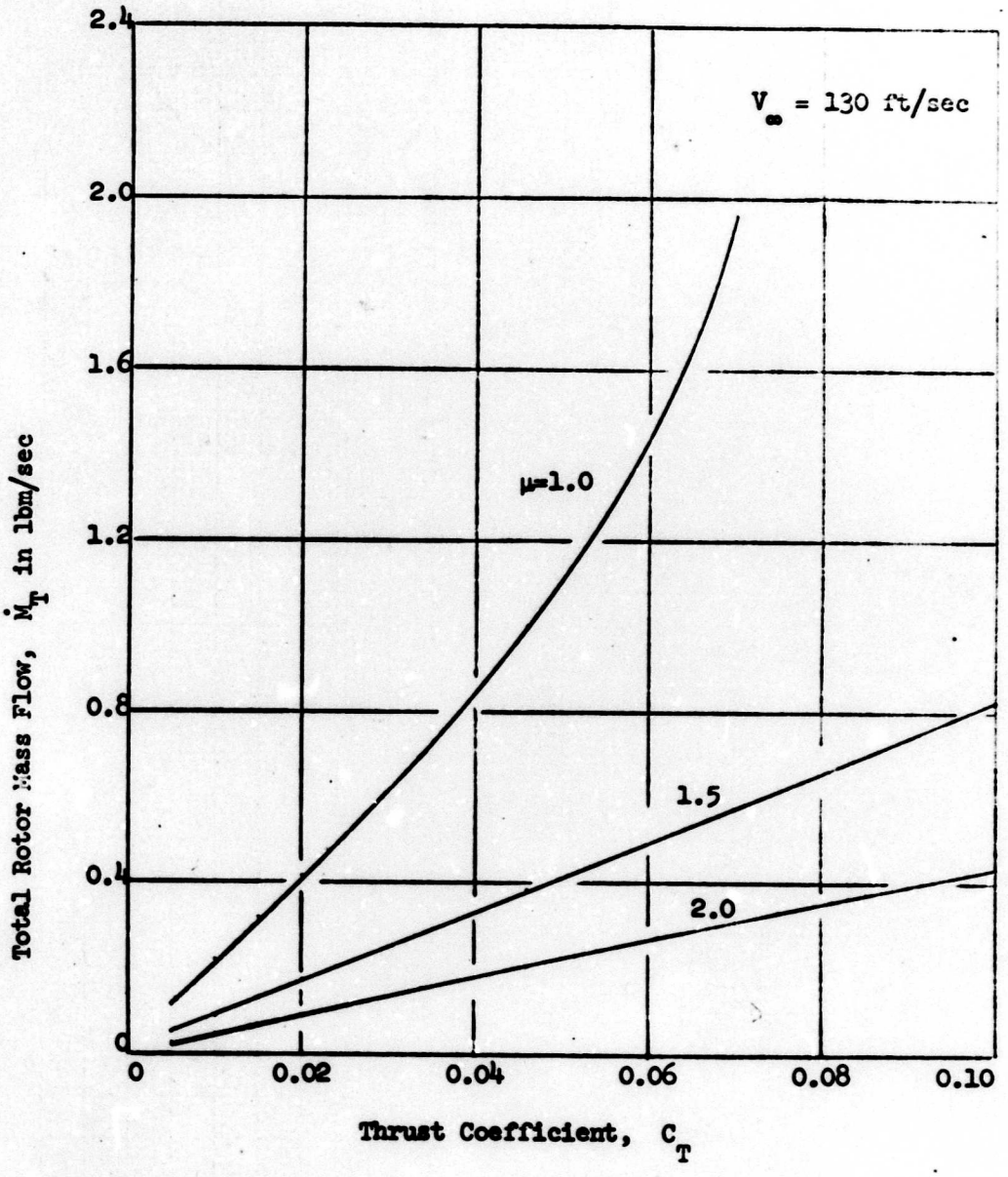

Figure 14 - Total Rotor Mass Flow Versus Thrust Coefficient

(a) V_∞ = 130 ft/sec

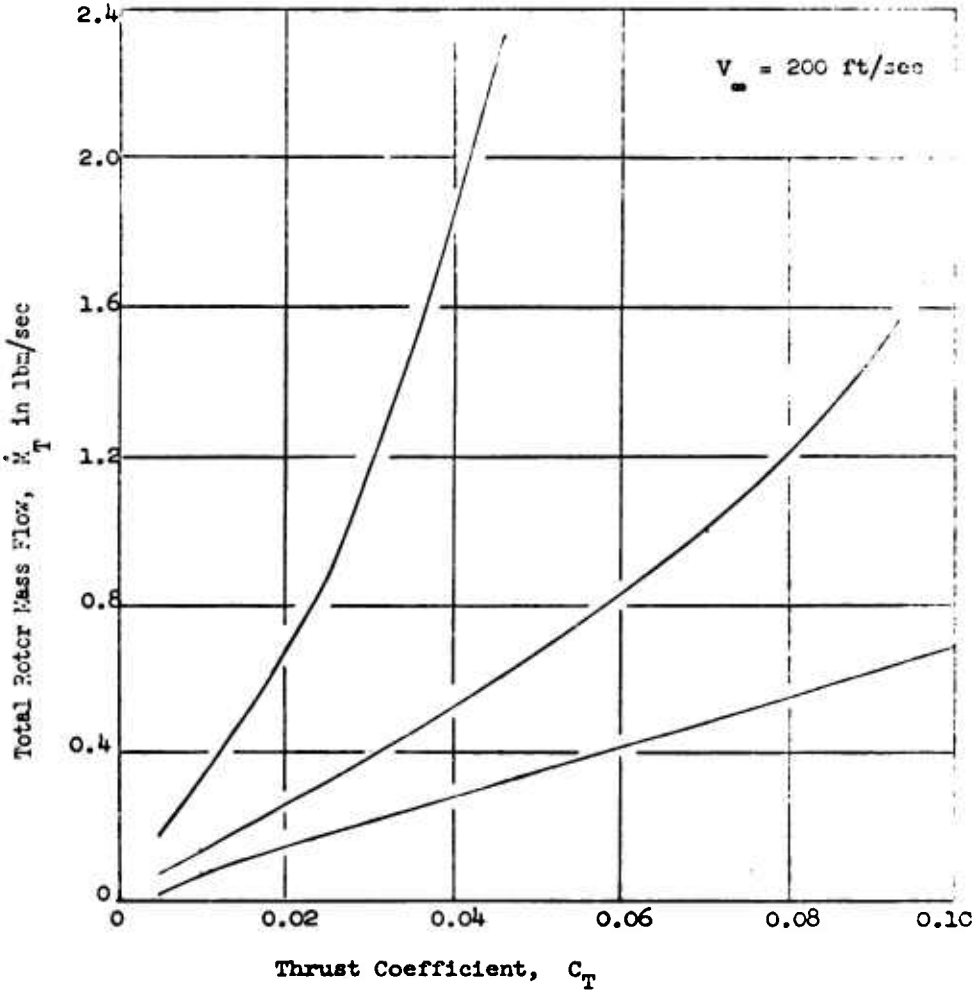

Figure 14 - (Concluded)

(b) V_∞ = 200 ft/sec

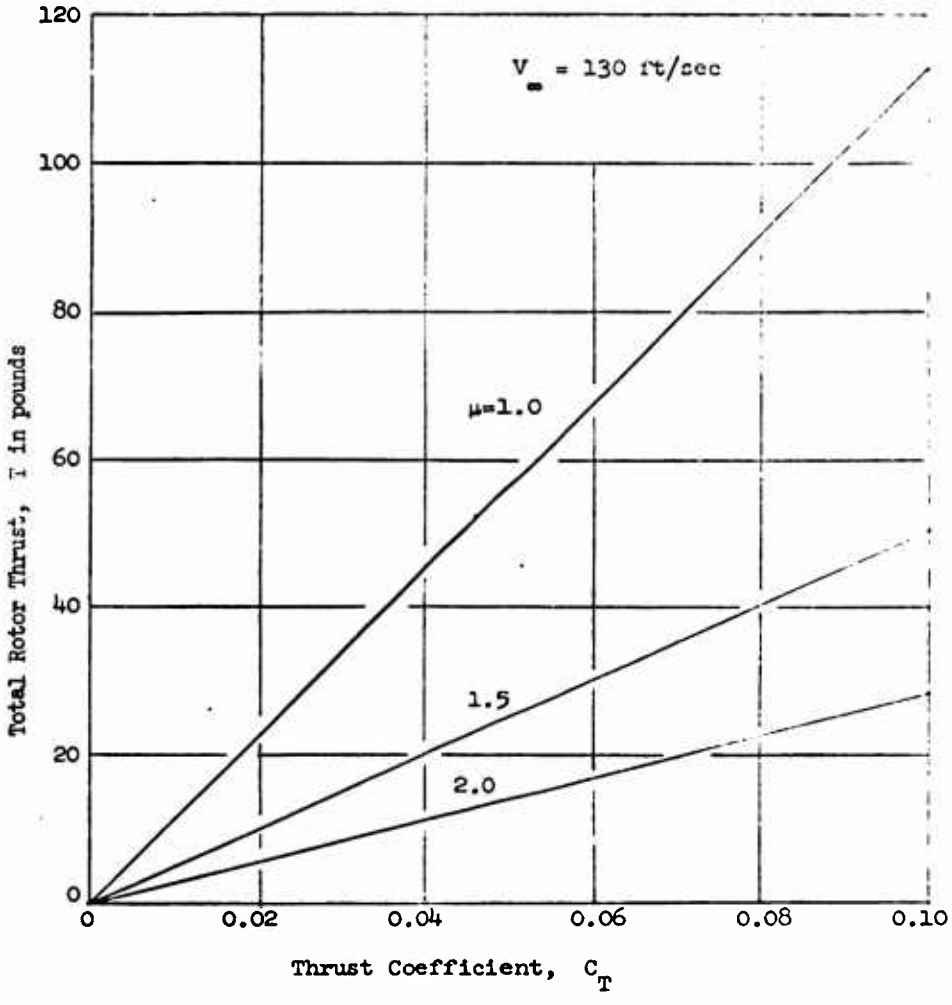

Figure 15 - Total Rotor Thrust Versus Thrust Coefficient

(a) V_∞ = 130 ft/sec

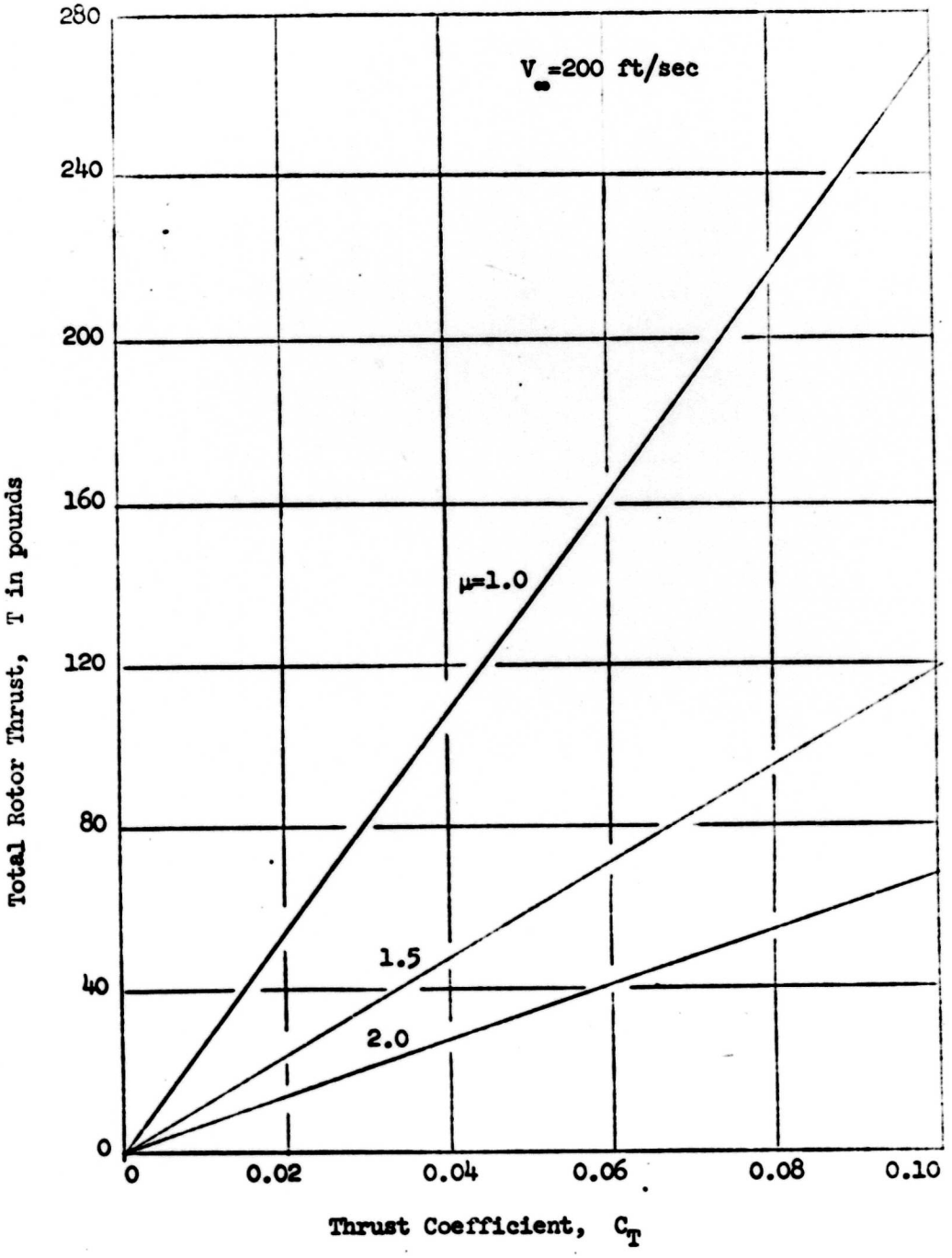

Figure 15 - (Concluded)

(b) V_∞ = 200 ft/sec

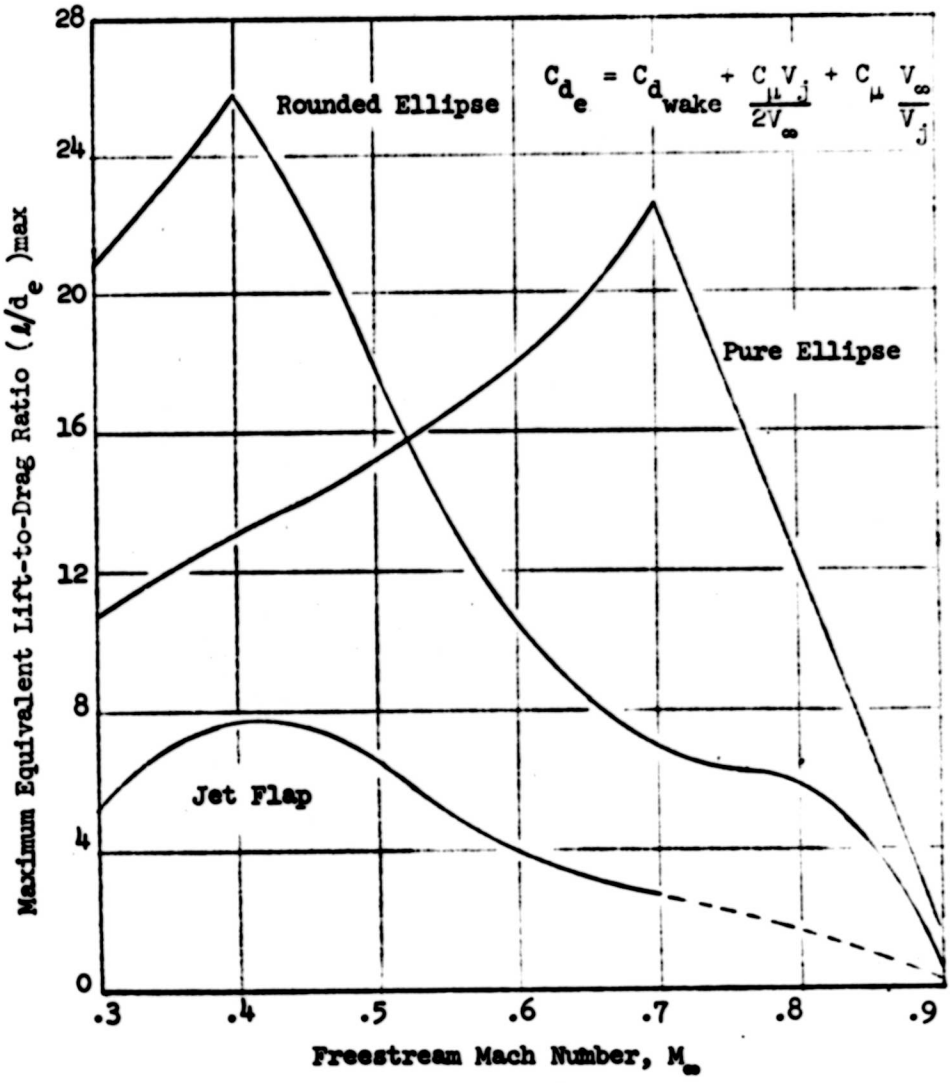

Figure 16 - Comparison of Maximum Kinetic-Energy-Based Equivalent Lift-to-Drag Ratio For Three Configurations

Table 1 - Range of Variables for Proposed Test

Variable	Testing Range
V_∞	130 and 200 ft/sec
μ	1.0, 1.5, and 2.0
C_T	0 to 0.10
N	200 to 650 RPM
T*	0 to 120 lbs.
$\dot{m}_T$*	0 to 2.2 lbm/sec
P_A*	14.7 to 18 psia
P_R*	14.7 to 50 psia
Q_s*	-30 to +120 in-lbs.
HP_c*	-.2 to 1.5

*Estimated values within ± 20%